CZECH TECHNICAL UNIVERSITY IN

PRAGUE

Faculty of Mechanical Engineering

Department of Automotive, Internal Combustion Engines and Rail

Vehicles

Study Program: Master of Automotive Engineering

Field of Study: Advanced Powertrains

Variance in nanoparticle emissions over WLTP Brake wear testing procedure

September 2022 Author: Praneet Ayyagari

Supervisor: Prof. Michal Vojtisek, M.S, Ph.D.

MASTER'S THESIS ASSIGNMENT

I. Personal and study details

Student's name: **Ayyagari Praneet** Personal ID number: **482805**

Faculty / Institute: **Faculty of Mechanical Engineering**

Department / Institute: **Department of Automotive, Combustion Engine and Railway Engineering**

Study program: **Master of Automotive Engineering**

Specialisation: **Advanced Powertrains**

II. Master's thesis details

Master's thesis title in English:

Variance in nanoparticle emissions over WLTP brake wear testing procedure

Master's thesis title in Czech:

Variabilita emisí nano ástic z ot r automobilových t ecích brzd b hem zkušebního cyklu WLTP

Guidelines:

The thesis is addressing the topic of nanoparticles originating from wear of automotive friction brakes. The goal of the thesis is to analyze particle concentration and particle size distribution data measured online during multiple runs of WLTP procedure, and possibly additional test sequences and/or "degreening" (bedding, break-in, conditioning) runs, with different types of front-wheel automotive disc brakes. The questions of distinguishing the instrument signal from each braking event from background concentrations and instrument noise, practically attainable detection limits, and repeatability of measurements over multiple test runs are to be addressed, including critical analysis, discussion and recommendations.

Bibliography / sources:

Grigoratos, T., et al. (2020). Atmosphere, 11(12), 1309.
Mathissen, M., et al. (2018). Wear, 414, 219-226.
Vojtíšek-Lom, M., et al. (2021). Science of the Total Environment, 788, 147779.
Zum Hagen, F. H. F., et al. (2019). Environmental science & technology, 53(9), 5143-5150.

Name and workplace of master's thesis supervisor:

prof. Michal Vojtíšek, M.S., Ph.D. Department of Automotive, Combustion Engine and Railway Engineering FME

Name and workplace of second master's thesis supervisor or consultant:

Date of master's thesis assignment: **21.04.2022** Deadline for master's thesis submission: **12.08.2022**

Assignment valid until: _____

prof. Michal Vojtíšek, M.S., Ph.D. Supervisor's signature	doc. Ing. Old ich Vítek, Ph.D. Head of department's signature	doc. Ing. Miroslav Španiel, CSc. Dean's signature

III. Assignment receipt

The student acknowledges that the master's thesis is an individual work. The student must produce his thesis without the assistance of others, with the exception of provided consultations. Within the master's thesis, the author must state the names of consultants and include a list of references.

Date of assignment receipt	Student's signature

Declaration of Authorship

I hereby declare that the following thesis is my independent work and to the best of my knowledge. All information has been acknowledged in the text with list of

reference.

In Prague: 15-08-2022 Praneet Ayyagari

ABSTRACT

This master thesis deals with the evaluation of particle emissions from four samples consisting of a combination of two brake pads and two brake discs for the front wheel of a typical automobile with regard to various braking conditions. A full-scale inertia brake dynamometer was used to test the brakes and the newly developed WLTP Brake cycle for brake wear particle testing. The particle concentrations were measured online with EEPS and ELPI particle sizers sampling from an outlet duct of the dynamometer enclosure as well as using a CPC. Particle production over the course of 3 runs of the WLTP Brake cycle was measured and compared in order to address the repeatability of the experiment. The experiment resulted in a good degree of repeatability between the samples and between consecutive runs of the drive cycle. The same consistency was also seen during the bedding-in process for one sample. The particle emissions during the WLTP brake cycle representing real driving were lower than the current exhaust PN emissions limit as a comparison.

Keywords: brake-wear, disc brakes, non-exhaust emissions, particle emissions, brake wear particles, WLTP Brake Cycle

ACKNOWLEDGMENT

First, I would like to thank God Almighty for his blessing and strength granted upon me and my family. Also, I would like to give my respect and love to my parents for all their supports and prayers during my entire life. I would like to express my sincere gratitude to my supervisor Prof. Michal Vojtisek, M.S, Ph.D., Faculty of Mechanical Engineering, Czech Technical University, Prague for his guidance, opportunities and patience provided in completion of the thesis work. Besides my supervisor, I would also like to extend my gratitude to doc. Ing. Martin Pechout, Ph.D., Faculty of Technology, Czech University of Life Sciences, Prague for his consultations and for all the help that was needed to understand this study. I would also like to extend my gratitude to the Czech Science Foundation for providing the fundings for the experiments under their project GA19-04682S. And finally, I would like to thank my beloved friends for their supports and prayers throughout my studies.

AYYAGARI PRANEET

Table of Contents

1. INTRODUCTION

The effects of air pollution is associated with over 7 million premature deaths annually, with over 4 million of such cases resulting from outdoor air pollution as reported by the World Health Organization (WHO). Air pollution is a mixture of various gases such as carbon monoxide (CO), sulphur dioxide (SO_2), nitrogen oxides (NOx), ozone and particulate matter (PM) with diameters ranging from few nanometres to hundreds of micrometres. The WHO also reports that PM, within which, the $PM_{2.5}$ emissions in particular, is one of the major pollutants in the air which have adverse effects on environment and human health, being associated with a large share of the cases reported above. [1]

Particulate matter is pervasive in the air and known to cause life threatening health effects and changes to the climate. Furthermore, the damages to human health caused by PM emissions from road traffic can be disproportionately large relative to other sources of PM emissions, as the highest emission levels tend to be localised in areas with the greatest population density, leading to high levels of exposure.[2] PM is composed of a complex mixture of particles of various sizes and compositions, with road vehicle emissions being a significant source of PM in metropolitan regions.

Particulate matter concentrations are of great concern due to a vast majority of populations being exposed to levels above the quality standards set by the WHO. The share of EU urban

population exposed to different air pollutants is shown in Figure 1, where it is seen that a significant portion of the population is exposed to both coarse and fine particulate matter.

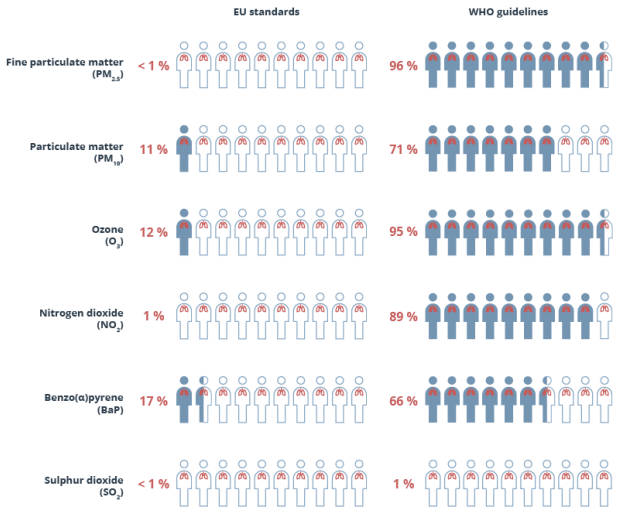

Figure 1. Share of urban EU population exposed to air pollutant concentrations over the EU and WHO guidelines in 2020 [3]

PM originating from combustion engine vehicles can be classified under two principal classifications based on its source: exhaust originating (e.g., vehicle tailpipe), coming about because of incomplete combustion and oil volatilization during ignition, and non-exhaust originating, made by vehicle component wear processes (e.g., brakes, tires, and resuspended road dust). Regulations on exhaust based emissions have been increasingly tightening which only leads to a growing importance of the contribution from non-exhaust sources to assess total traffic related particulate emissions, with the overall share of brake wear particles adding up to traffic-related PM increasing with time. While the measures to curb exhaust PM emissions have been largely effective, they do not regulate PM emissions from electric vehicles, and although they have been widely supplied to the global market, the contribution presently of EVs to total PM is comparable to that of internal combustion engine vehicles (ICEVs) because EVs generate more tire-road wear particles, as well as resuspended road dust, than ICEVs due to their increased weight.[4] There have been studies which have dealt with finding a novel cycle to provide the means to test the emissions from brake wear and a version

of the Worldwide Harmonized Light Vehicles Test Procedure (WLTP), currently a global standard for testing exhaust emissions and fuel consumption of vehicles with all varieties of powertrains, was utilised to design a drive cycle to simulate brake wear emissions. With no legislative standards to regulate the non-exhaust PM emissions presently, with the novel drive cycle serving as a benchmark, some regulatory guidelines may be established. [studies

1.1 Ambient Air Quality

Ambient air quality standards have been set by governmental agencies and health organizations worldwide to regulate the levels of pollutants in the atmosphere. Standards set by the EU and WHO for particulate matter are shown in Table 1. [3]

Table 1. PM emission limits by the EU and WHO.

Pollutant	EU Limit Values	WHO
PM_{10}	50μg/m^3 (1 day)	45μg/m^3 (1 day)
	40μg/m^3 (annual)	15μg/m^3 (annual)
$PM_{2.5}$	25μg/m^3 (annual)	5μg/m^3 (annual)

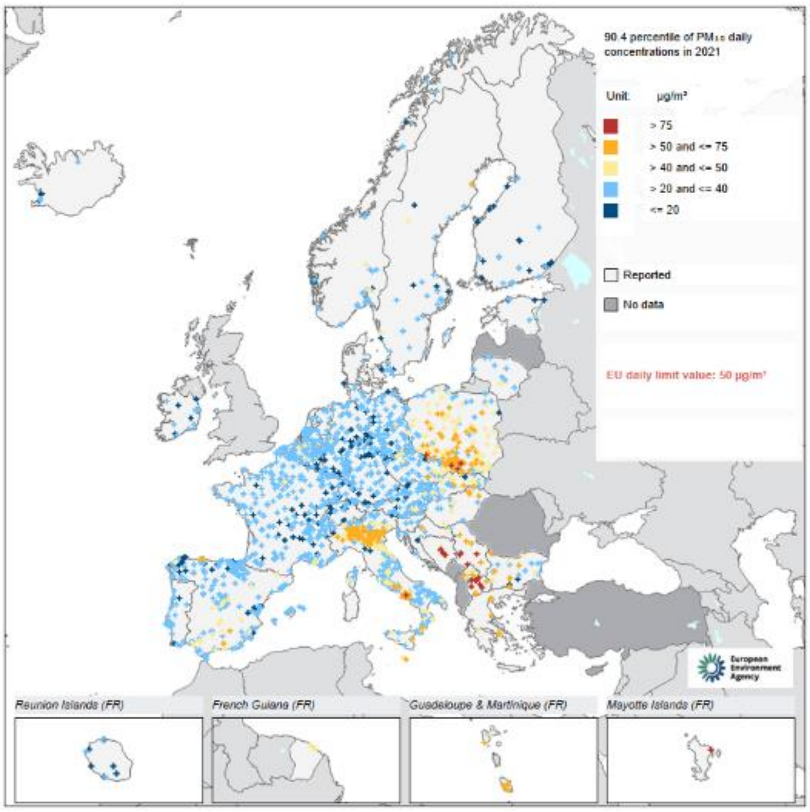

Figure 2. PM10 concentrations in EU member states [3]

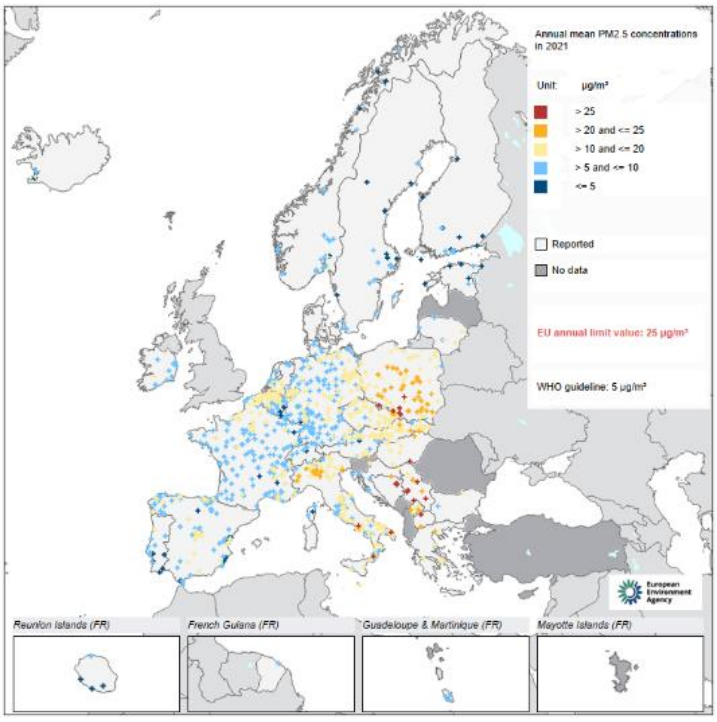

Figure 3. PM2.5 concentrations in EU member states [3]

Figures 2 and 3 show the reported concentrations of PM_{10} and $PM_{2.5}$ respectively. Concentrations of PM_{10} above the EU daily limit value were measured at 16% of monitoring stations, 84% of which were urban and 11% suburban, whereas those of $PM_{2.5}$ above the EU annual limit value were registered at 2% of monitoring stations, 69% of which were urban and 21% suburban. It is seen that urban areas (95% for PM_{10} and 90% for $PM_{2.5}$) have been affected significantly more than rural areas.

1.2 Particulate Matter Origin

It is a complex mixture and can vary greatly in size, composition and the nature of formation They can be directly emitted from the sources or indirectly from the gaseous pollutants already in air which turns into particulate matter. Therefore, it is grouped into primary and secondary particles.

Primary particles are emitted from sources such as road vehicles, heavy machineries, mining, construction and burning activities (e.g. burning of wood, forest fires etc.). Secondary particles are formed in the air due to the intermediate reactions of gases such as sulphates, nitrates and carbon containing reactive organic gases. [5]

Particulate Matter can originate from both the exhaust gases in the form of soot, or from non-exhaust sources. These can be broadly classified under:

- Brake assembly wear (brake disc/drum and pads).
- Tire wear.
- Resuspension of road dust.

The amount of PM generated by each vehicle is determined by factors including the vehicle weight, materials of the brake components (brake pads, disc, callipers), the driving surface, amount of dust already on the road, and driving styles.

1.3 Particulate Matter Classification

Particles are broadly classified based on their particle diameter (Dp). They are:

- PM_{10} – coarse (Particles with $D_p \leq 10$ µm)
- $PM_{2.5}$ – fine (Particles with $D_p \leq 2.5$ µm)
- $PM_{0.1}$ – ultra fine (Particles with $D_p \leq 0.1$ µm)

Figure 4 shows the classification of PM and the common sources associated with the generation of each sub-type of particle sizes. [6] Coarse particles are the particles between PM10 and PM2.5 and PM10 refers to all the particles of size diameter below 10µm. They are formed from the mechanical break-up of larger particles and settle down without being displaced too much in the air. These include most visible forms of particles such as soil, dust from construction and mining operations etc.

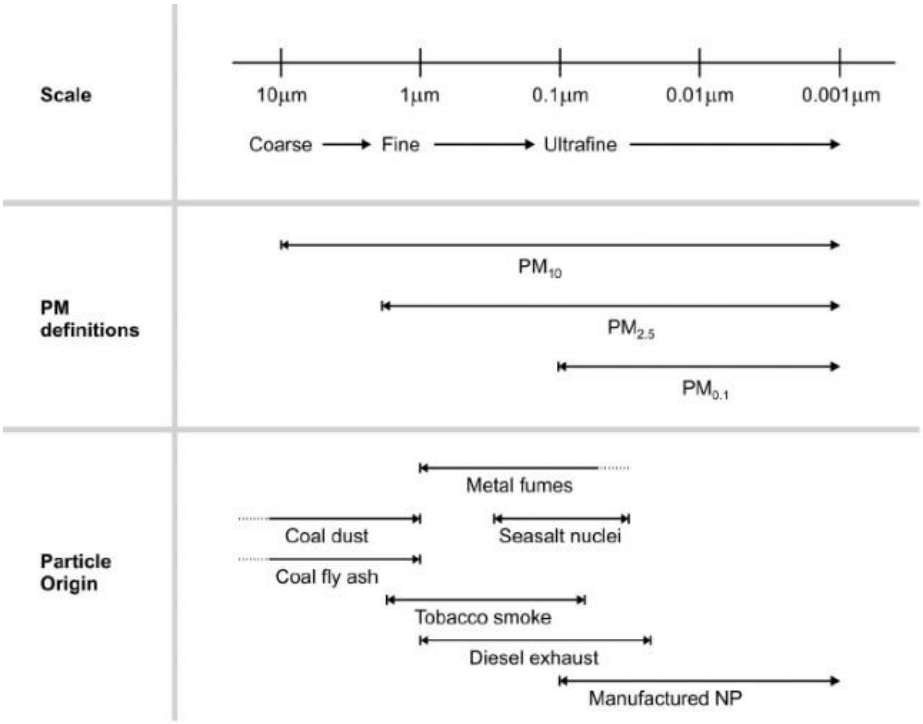

Figure 4. Particulate Matter size classification and common sources [6]

Fine particles or PM2.5 are also known as respirable particles which can travel to the respiratory tract. They are generated from primary sources such as combustion and formation of secondary particles through condensation and coagulation.[7] Ultra-fine particles (UFPs) are those with particle diameter less than 0.1μm and are unstable. They grow into larger particles by coagulating and condensing and dominate the surface area of particulate emissions. Due to their extremely small sizes, they can penetrate far deeper into the respiratory system and cause severe health issues. Figure 5 shows the level to which the various sizes of particles can penetrate into the respiratory system. [8]

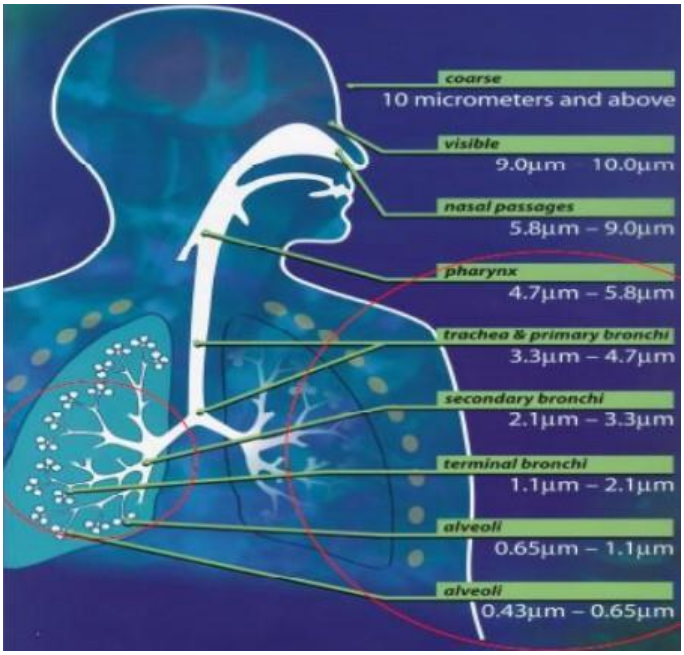

Figure 5. Penetration of various PM into the human respiratory system [8]

Concentration of airborne particulate matter is often characterised by PM10. Under certain friction conditions car brake materials emit ultrafine particles (with diameters below 0.1 µm) These particles have a number concentration several orders of magnitude higher than that of fine particles. This implies that their mass contribution to PM10 can be considerable. [9][10]

1.4 Non-exhaust PM Emissions

Non-exhaust particle emissions from road traffic consist of airborne particulates generated by the wearing down of brakes, clutches, tyres and road surfaces, as well as by the suspension of road dust. The relative contribution of each source to the total particulate emissions can differ significantly across different vehicle types. Figure 6 shows the contribution of different sources in the emissions taken from a study in a high urban population and vehicular density

city of Delhi as an example to illustrate the overall large share of non-exhaust sources in the total emissions.

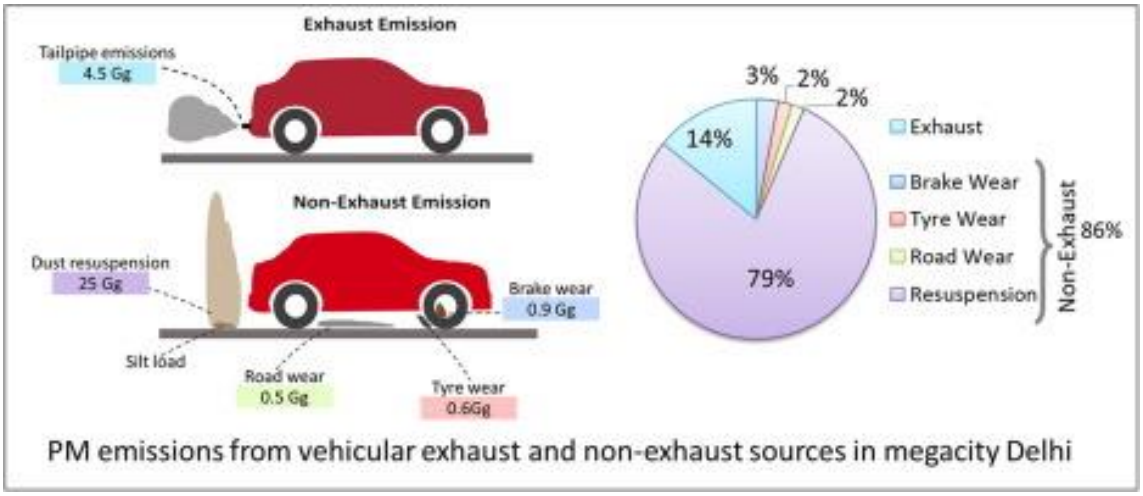

Figure 6. PM Emissions from exhaust and non-exhaust sources in Delhi [11]

1.4.1 Tyre Wear Emissions

Tyre wear emissions are generated due to the interaction between the tyre and road surface which causes abrasion of the tyre tread. Tyre wear particles are composed of plasticizers, oils, polymers, carbon black and minerals. [12] The effect of these particles has been reduced since the elimination of Polycyclic Aromatic Hydrocarbons (PAH) from tyres in the EU by the REACH regulation.

The average passenger vehicle tyre has a life of 40,000-50,000 km, with 10-30% of its tread rubber emitted to the environment. The amount of material lost varies depending on the characteristics of the tyre, vehicle, and road surface, as well as the vehicle operation conditions. [13]

Tyres contain a wide range of chemicals suited for different performance requirements. Tread components consist of blends of different rubbers (41%) compounded with fillers

(30%), reinforcing materials (15%), plasticizers (6%), chemicals for vulcanization (6%), and anti-aging agents (2%).[14]

1.4.2 Road Dust Emissions

Road dust is a generic description for any form of solid particles distributed along the road surface that can potentially be resuspended in the air through traffic or wind. Several sources for this road dust include particles from traffic-related wear, construction sites, depositions from exhaust gases, migrated particles from nearby environments, and deposition from the atmosphere. [15]

Road dust emissions from vehicular non-exhaust sources vary significantly depending on the condition of the road surface, vehicle speed, driving style, and surface texture.

1.4.3 Brake Wear Emissions

Braking is considered to be a major source of non-exhaust traffic emissions, particularly in urban and sub-urban areas. Brake wear PM are generated during the friction between brake pads and discs (or shoes, in drum brakes). Brake wear contributes up to 20% of total traffic emissions [16], and approximately 50% by weight of the wear debris became airborne within all the vehicles tested in a study. [17] The chemical compositions of the brake lining varies between manufacturers but contain concentrations of different metals which can be fatal with long term exposure. Figure 7 shows the average concentrations of commonly found metals in brake pads and discs.

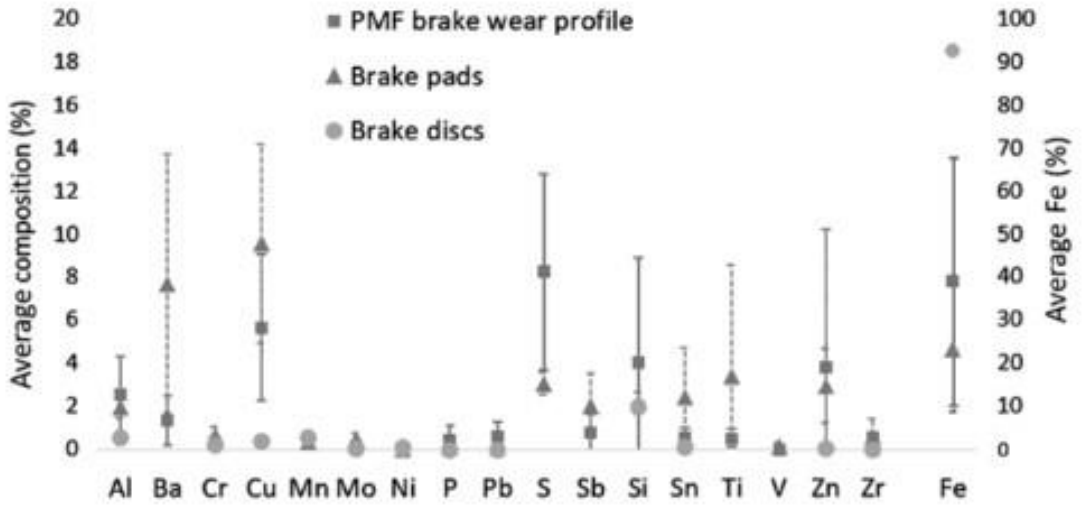

Figure 7. Average compositions of brake pads, brake discs and positive matrix factorization of brake wear profile [15]

The particles originating from the wear, also called Brake Wear Particles (BWP), are discussed in the next sections.

1.5 Brakes

The purpose of the braking system is to assist the vehicle in slowing down or come to a complete stop. The kinetic energy of the vehicle is dissipated as heat by the brakes. Friction is the fundamental principle behind the functioning of the braking system.

Two braking mechanisms have been widely utilized in present day automobiles: disc brakes, in which brake pads housed in a calliper are clamped against a rotating disc, and drum brakes, in which curved brake shoes are forced against the internal surface of a rotating cylinder or drum. Modern brake systems have employed the brake disc configuration with the drum brake design reducing in use. It is assessed that front brakes need to give around 70 % of total braking force, and are more stressed under braking due to the vehicle load transfer to the front axle and consequently must be replaced more regularly than back ones. Rotors utilized

in automobiles are generally made of grey cast iron or stainless steel, however, ceramic matrix composites such as carbon fibre reinforced silicon carbide (C-SiC) , and aluminium have also been used for high performance applications. [18] An example of a typical disc and drum brake is shown in Figure 8.

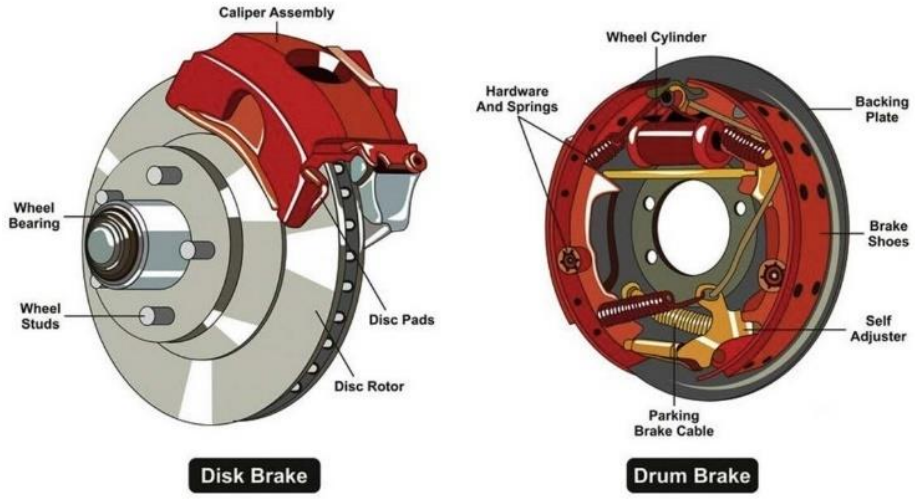

Figure 8. Disc and Drum brake assembly [19]

1.5.1 Brake Wear Particles

The rate of the brake wear depends on the composition of the linings and the operating conditions of the brake which subsequently influences the chemical and physical properties of the emitted particles. [20]

Braking is considered to be one of the major sources of non-exhaust traffic related particle emissions especially in urban areas and could contribute around 16-55 % by mass to total non-exhaust particulate emission [21]. One of the experiments conducted on brake dynamometer with different brake linings show that 86% of brake wear particle mass concentration was distributed in fine PM2.5 and 63% in Ultrafine particulate matter in PM0.1

(UFPs) region [9]. This can be due to the volatilization of the brake material which could condense in the air and therefore form fine particulate matter.

The exact composition of the individual components varies across the linings and its intended application. Moreover, complete composition data is not fully disclosed by the manufacturers due to proprietary rights. So, typically, brake linings generally comprise of five major components [20]:-

- ***Fibres***: Provide mechanical strength by reinforcement and account for 6-35 % of the brake lining mass. Fibres of carbon, glass, minerals are frequently used.

- ***Abrasives:*** Helps to increase friction and hinders built-up of heat transfer films which will reduce braking efficiency. Around 10% of lining mass is comprised of abrasives. Oxides of Al, Fe, Quartz are usually employed.

- ***Lubricants:*** It contributes 5-29 % of lining material and help in stabilizing frictional properties at high braking temperatures. Common materials used are graphite and metal sulphates.

- ***Fillers:*** They help in reducing manufacturing costs and improve manufacturability of the brake linings. Typical materials used are barite ($BaSO_4$) and mica and contribute 15-70% to lining.

- ***Binders:*** This component holds all the components together which is to retain the structural integrity of the lining. Phenolic resins are extensively used with variation of 20-40% depending on the required performance.

The wear generated from disc brakes originate from contact between the pad and disc. In a model the contact between an organic brake pad and a cast iron disc, it was seen that the hard material fibres in the pad material form stable primary contact patches with the disc and carry the bulk of the load. The wear particles originating from the disc and the pad flow in the boundary layer between the pad and the disc, enabled by large enough gaps between the primary patches. These particles can also accumulate around the primary patches and form secondary contact patches while the remaining particles will escape to the surroundings. These patches are unstable and changes in the contact situation between the pad and the disc can dislodge the secondary patch and allow the accumulated particles to break loose. [22]

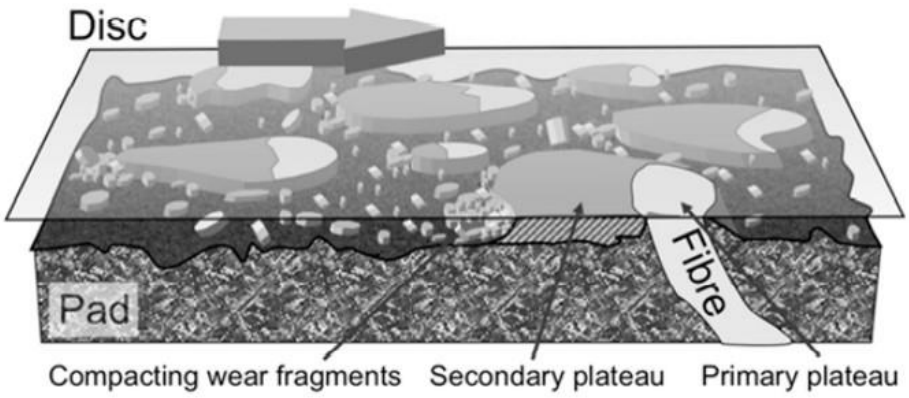

Figure 9. Contact between brake pad and disc showing the primary and secondary plateau (or patches) and the flow of wear particles between the gaps [23]

Figure 9 shows an illustration of this contact situation. The primary patches between the fibres and the brake disc, along with the flow of particles in the gaps and accumulating to form secondary patches is seen clearly. The measured particle emissions from brake wear originate due to the frictional contact of the brake pads with the disc but they are not all released when the brake is applied, i.e; brake wear particles were not only observed during braking but also during driving when the brake was fully released, which includes a short interval after the brake is released and there is still some contact between the surfaces (also called brake drag) and also a short duration after the contact is fully removed. [23] This is explained by the breaking down of the secondary plateaus to release the BWPs to the surroundings when the brake pad disengages.

1.6 Objective of the thesis

The thesis addresses the topic of ultrafine or nanoparticles that are generated as a consequence of brake wear. The objective of this thesis is to analyse the particle concentrations and particle size distribution data generated during multiple runs on the WLTP cycle of 4 different types of front-wheel automotive disc brakes. The data was measured using 3 instruments, a Condensation Particle Counter (CPC), an Engine Exhaust Particle Sizer (EEPS) and an Electrical Low- Pressure Impactor (ELPI). Also addressed in this thesis are:

- Distinguishing the instrument signal of each braking event from the background concentrations and noise.
- The repeatability of these measurements taken over multiple runs of the WLTP cycles.

2. EXPERIMENTAL AND INSTRUMENTATIONAL SETUP

The tests were carried out on a brake dynamometer with four different types of front-wheel automotive brake discs. Each sample underwent multiple runs of the WLTP test cycles and the wear particles were measured using a Condensation Particle Counter, an Engine Exhaust Particle Sizer, and an Electric Low-Pressure Impactor. The dynamometer and the instruments used are discussed further. All brake discs and pads used for the experiment were new and hence also had to undergo a bedding-in process before the measured runs took place.

2.1 Testing Schedule

The tests were conducted on 4 samples consisting of various combinations of 2 different brake pads and 2 different brake disc materials. All the tests were done at the laboratories of Technical University of Ostrava in the month of February and March of 2022. Each sample was tested for an extensive period, undergoing multiple runs of the WLTP cycle for the bedding-in process as well as the emissions testing runs. Testing took place from 14th February 2022 until 5th March 2022.

Table 2 shows the schedule of the tests performed.

Table 2. Testing Schedule

Sample	Sample 1	Sample 2	Sample 3	Sample 4
Bedding-In Run (5 WLTP-Brake cycles)	14.02.22-15.02.22	17.02.22-18.02.22	01.03.22-02.03.22	03.03.22-04.03.22
Emissions Run (3 WLTP-Brake cycles)	28.02.22-01.03.22	21.02.22-22.02.22	02.03.22-03.03.22	04.03.22-05.03.22

2.2 Brake Dynamometer

The wear and durability of the braking system is assessed with the help of certain standardized test procedures to estimate the wear life of the friction pair at the design stage. Real world tests involving a full vehicle on the road with emissions measured by mobile units are also performed, however the former is having the advantage of conducting tests in a reproducible manner, while preserving the brake as a full system: Test procedures that include environmental conditions, drive cycles, and vehicle load (inertia), are easily constrained. Although dynamometers are the basis for robust measurements, the methods of sampling and measuring brake wear particles deviate widely. Dynamometer tests also have the advantage of being able to run for a long period of time to simulate and measure the performance of the brake over its lifetime.

The dynamometer consists of the following sections: [24]

- Drive Section

  The motor provides the torque to turn the brake assembly to simulate the vehicle's forward driving kinetic energy. The dynamometer drive motor also provides the required torques for drag conditions and for simulation of grade effects from mountains to driveways.

- Inertia Section

  The inertia section of a brake dynamometer is responsible for simulating the mass and inertia of a vehicle. This section of the dynamometer has large discs that resemble flywheels in appearance and function. By varying the number of these discs the inertia and mass for a vehicle can be simulated. These discs are then driven by the motor and provide the stored energy for decelerating conditions during testing.

- Test Bed

  The output shaft of the inertia section terminates in the enclosure, test bed or cell. The rotor and caliper may be mounted to an actual knuckle, or a jig that can hold the components. Typically the output shaft is attached to the rotor or drum where the wheel attaches.

Testing of modern composite friction materials consists of a series of repetitive braking scenarios from a set speed and temperature range. This approach serves as the basis for comparison of different friction materials under similar conditions. Tests on the 4 samples of brake discs were run in the laboratory from 16.02.2022 to 05.03.2022

Front brake assembly with original calliper and the sample brake disc was coupled to a full scale brake dynamometer as shown in Figure 10. The rotor is coupled by a rotating shaft to an asynchronous electric motor and a flywheel. The assembly is accelerated to the desired speed by the motor. When prescribed conditions are reached such as temperature, hydraulic

pressure in the brake lines are regulated via actuator to match the target brake line pressure or deceleration rate. The rotor is coupled to the flywheel simulating vehicle translational and rotational inertia corresponding to approximately 35% of the vehicle equivalent test mass (with a 70-30 brake force distribution between the front and rear wheels). Thermocouple inserted in a hole drilled radially into the rotor measured the temperature of the rotor.

Figure 10. Experimental Setup of the brake disc on the dynamometer

The rotor and the brake assembly are housed in an airtight enclosure as shown in Figure 10, through which air was circulated by fans a flow rate of 2400 m^3/ hr to provide cooling for the brake assembly and to scavenge fumes and smaller brake wear debris from the enclosure.

2.2 Instruments Used

Online Particle size classifiers are employed at the test facility to measure particles emitted from the brake assembly during and after the braking event. Dekati Electrical Low-Pressure Impactor (ELPI+) and TSI Engine exhaust particulate size spectrometer (EEPS) along with a Condensation Particle Counter (CPC) are the ones used in this experiment to measure PM.

2.2.1 Engine Exhaust Particle Sizer (EEPS)

EEPS is fast response and high-resolution particle measurement instrument having capability of measuring the particles of size in the range 5.6-560nm. The particles entering the instrument are positively charged to a predictable level at the inlet with the help of corona charger and are transported downstream with help of filtered sheath air [25].

The classification of particle is based on differential electrical mobility. When the charged particles enter the column above the central electrode as shown in Figure 11, the particles are deflected radially outward and collected on the electrically isolated electrodes.

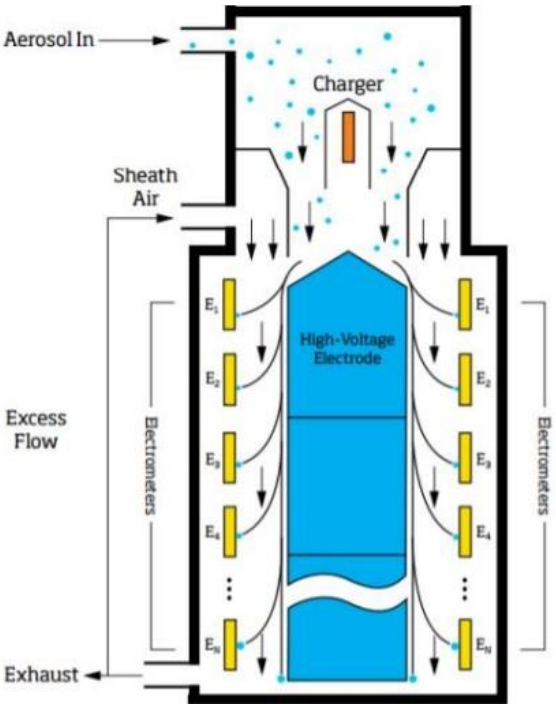

Figure 11. Schematic diagram of an EEPS [25]

The particles with high electrical mobility are deflected to the electrode at the top and the with lower mobility comes further to the downstream. The electrodes are connected to a sensitive charge amplifier known as electrometer. To synchronize the time delay between

electrometers, variability in charge of the particles, and size distribution with respect to time, the EEPS utilizes a built in Digital Signal Processor (DSP) [25].

2.2.2 Condensation Particle Counter

Condensation Particle Counters are used to count particles of a wide range of sizes down to 2 nm, depending on the specific models. Particles are detected and counted by first enlarging them by using these particles as nucleation centres to create droplets in a supersaturated gas. CPCs are of special importance due to their ability to detect particle sizes of less than 50 nm, which are generally undetectable with conventional optical counters.

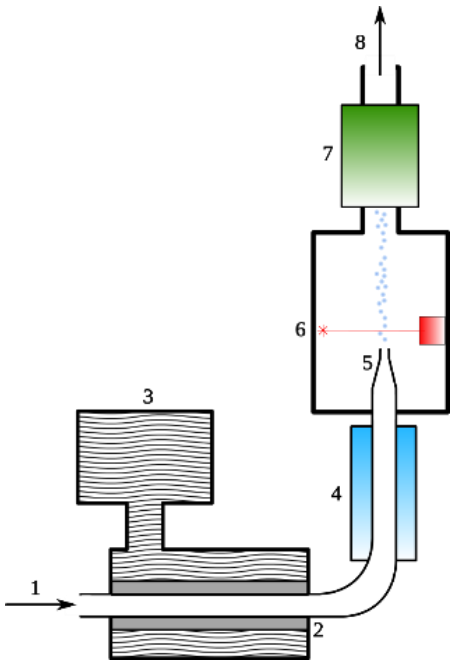

Figure 12. Schematic of CPC [26]

Figure 12 shows the schematic of a CPC with the notation as follows: 1 – air inlet; 2 – porous material block, 3 – working fluid in reservoir, 4 – condenser, 5 – focusing nozzle, 6 – laser-based counter, 7 – air pump, 8 – air exhaust. In a supersaturated vapour suspended particles

act as nuclei for vapour condensation and may grow to form droplets. This process is referred to as heterogeneous nucleation. Above a critical supersaturation droplets may form by homogeneous nucleation where clusters of vapour molecules nucleate droplets.

Air passes through a hollow block of porous material in contact with the working liquid, the block being heated to ensure high vapour content. Then the humified air enters the cooler where nucleation occurs. Temperature difference between the heater and the cooler determines the supersaturation, which in its turn determines the minimal size of particles that will be detected. The more uniform is obtained supersaturation, the sharper is particle minimal size cut-off. During the heterogeneous nucleation process in the nucleation chamber, particles grow up to 10-12 µm large and so are conveniently detected by usual techniques, such as laser nefelometry (measurement of light pulses scattered by the grown-up particles)

2.2.3 Electrical Low- Pressure Impactor (ELPI+)

ELPI+ is used to measure real time particle size and concentration in the size range of 6nm-10µm. The instrument classifies particles into 14 size classes depending on the aerodynamic size of the particle (Dp). The particles are charged with the corona charger before entering series of cascade impactors. The principle of inertia makes the particles to settle down on the respective impactor stages [27].

A schematic of the ELPI+ is shown in Figure 13.

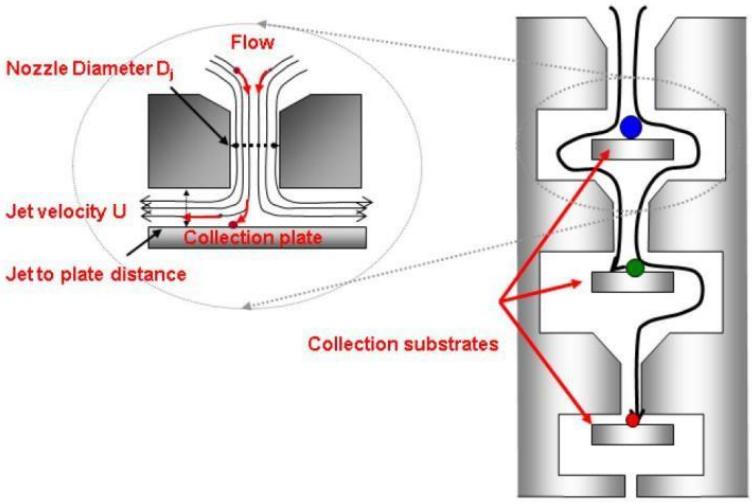

Figure 13. Schematic of ELPI+ [27]

The particles larger than certain aerodynamic size get collected on the upper impactor stages and smaller ones travel down to the lower stages and get settled. This is due to of particles larger than certain aerodynamic diameter resist to take a turn and settle down on the impactor while smaller particles remain in the flow. The electrometers attached to the corresponding impactor stages detect the charge carried by the particles [27]

3. BRAKE WEAR TEST PROCEDURES

The wear and durability of the braking system is assessed with the help of certain standardized test procedures to estimate the wear life of the friction pair at the design stage. This is carried out using some laboratory based methods rather than vehicle based due to cost and time constraints. Testing of modern composite friction materials consists of a series of repetitive braking scenarios from a set speed and certain initial temperature range. This approach serves as the basis for comparison of different friction materials under similar conditions. Therefore, to assess the wear of the four discs, they were put through multiple runs of the standardized test protocol for brake testing, the WLTP- Brake cycle. Some standardized brake wear testing procedures typically comprise a range of extreme events, including a simulation of brake fading during prolonged hill descent and during repeated hard stops from very high speeds. These tests are intended to assess the brake performance during most extreme conditions, which are rarely encountered during ordinary operation.

The regulating bodies governing these standardised tests are:

- Federal Motor Vehicle Safety Standards (FMVSS) and the National Highway Traffic Safety Administration (NHTSA) Regulations.
- Standards from Society of Automotive Engineers (SAE).
- International Standards from the International Organization for Standardization (ISO).
- Regulations from the United Nations Economic Commission for Europe (UNECE).

Some of the commonly used driving cycles for exhaust emissions and brake wear testing are: [28]

- WLTC (World Harmonized Light-duty Test Cycle)
- NEDC (New European Driving Cycle)
- FTP-75 (Federal Test Procedure)
- LACT (Los Angeles City Traffic)
- WLTP-Brake (World harmonized Light-duty Test Procedure for Brake emission)

Table 3 shows the test times, driving distances and number of braking events in each of the abovementioned cycles. The LACT test is modified to fit a 3 hour run for the purpose of assessing brake emissions.

Table 3. Comparison between different commonly used cycles for exhaust and brake emissions

Name	WLTC	NEDC	FTP-75	3h-LACT	WLTP-Brake
Purpose	Evaluating exhaust pollutant emission	Evaluating exhaust pollutant emission	Evaluating exhaust pollutant emission	Evaluating brake particle emission	Evaluating brake particle emission
Test Time	30 min	20 min	41 min	3 h	4 h 24 min
Driving Distance (km)	23	11	17.8	150	192
No. of Braking events	51	18	45	217	303
Braking frequency	2.22	1.64	2.54	1.45	1.6

3.1 WLTP Cycle

The WLTP database consists of in-use driving data from five different regions (EU, USA, India, Korea and Japan) with a total mileage of 743,694 km. The WLTP database was used to develop the worldwide harmonized emissions type approval test cycle for light-duty vehicles (WLTC) and was considered as the de facto standard for normal driving data. Using the WLTP database, a novel braking cycle, the WLTP brake cycle, was developed to reflect real world braking patterns, as a part of the proposed commonly accepted methodology for brake wear particles sampling and measurement. The WLTP brake cycle is divided into 10 segments and the soak time is adjusted such that the starting temperature of the disc is below a certain fixed temperature before start of each segment. [29]

This cycle has a total driving distance of 192 km with 303 braking events in each cycle. The cycle is divided into 10 segments with an adjusted soak time between segments to allow the brakes to cool. The Figure 14 shows the velocity vs time curve of the WLTP brake cycle, showing a maximum braking speed of 133 km/hr.

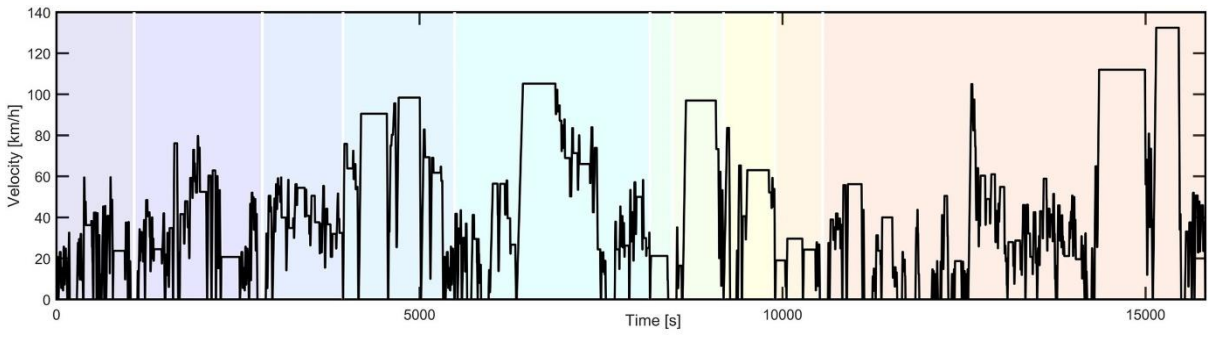

Figure 14. Velocity-time schedule of the WLTP Cycle

Before the measured runs took place, each of the 4 samples were subjected to the "degreening" or "bedding- in" process. This is a process recommended to be done on newly

manufactured brake discs and pads as a way to ensure optimal performance of the braking system.

The bedding- in process involves the transfer of an even layer of brake pad material on the surface of the brake disc, which assists in smoother brake operation and improved braking power. The process also serves to increase the effective contact patch between the pad and disc and by removing much of any unevenness of the contact surfaces results is a more uniform application of the brake pressure on the rotor.

The samples in this experiment underwent a rigorous bedding-in process consisting of 5 runs of the WLTP Brake cycle to ensure that the brake system is optimally functional while also simulating a sample resembling a real-world brake assembly.

4. ANALYSIS

The particle emissions recorded by the three instruments is extracted and analysed for useful data. Each response recorded by the instrument consists of the useful signal, which is the true response from the measured sample, and unwanted noise. [30] It is necessary to separate the signal from the noise to obtain the true emissions from the tested brake sample.

4.1 Signal and Noise

The strength of the measured signal should be distinguishable from the noise which is recorded along with the useful response. So, to quantify this, the noise needs to be separated from the useful signal to describe the performance of the instrument. The source of noise could be from within the instruments or from the influence of surrounding environment [31].

In general, net value of the signal can be calculated by removing estimated background from the recorded value. These background concentrations are often referred as 'noise' or the 'disturbance' in the signal. Noise can be divided in two categories- one, is Internal Noise which is associated with its own components; and the other is External Noise which is associated with the vibration or any physical disturbance to the instrument.

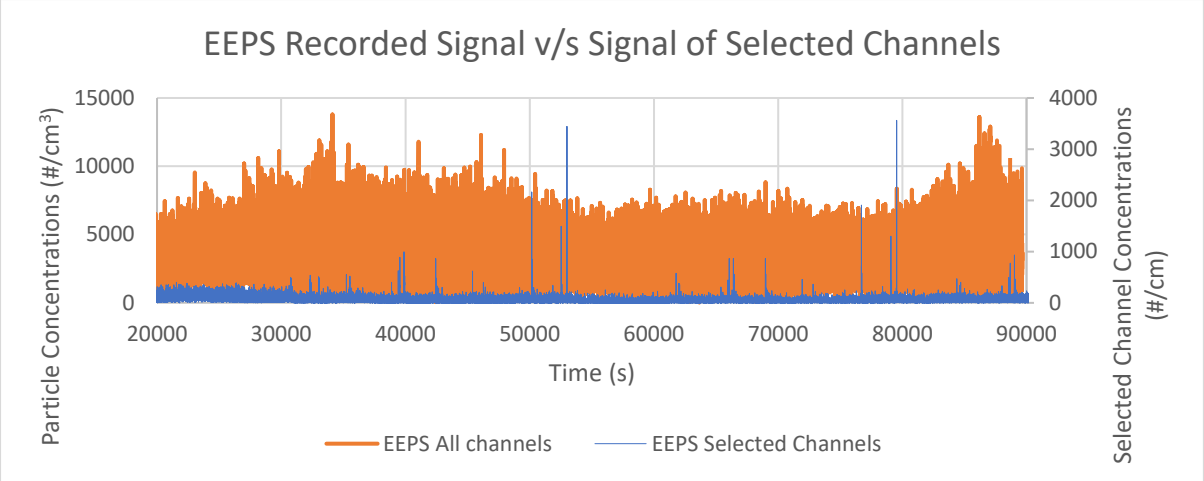

Figure 15. EEPS Signal with noise and from selected channels

Here, it was observed that the lower sized channels of the EEPS had been producing excessive noise which made it indistinguishable from the true useful signal for the particle concentrations in those channels as seen in Figure 15. Due to this issue, the concentrations reported from the distinguishable bins were reported and it is to be noted that the EEPS data represented in the discussion relates to the concentrations obtained from the distinguishable channels.

4.2 Synchronization of Instruments

The resolution time for all the instruments involved in the experiment is 1 Hz. However, the response recorded by the instruments for the corresponding brake event could be delayed sometimes due to various factors such as response time of respective instruments and length of sampling line. The timing of the brake event is recorded and is taken as a reference to check for the change in current/concentration values recorded in the instrument data sheets for the same time. It is observed that the instruments recorded the signal with a gap of 30 seconds

between their respective recorded times. So, both instruments had to be synchronized with braking time and then perform the analysis. The CPC and the EEPS both recorded the signals at the same time, as they are recorded on the same computer and did not require synchronization. This synchronizing is done to make sure that the responses recorded by the instruments are in line with the braking events performed on the dynamometer and measured value corresponds to the respective braking event shown in Figure 16 (Series 1 is the signal from the ELPI and Series 2 is the signal from EEPS).

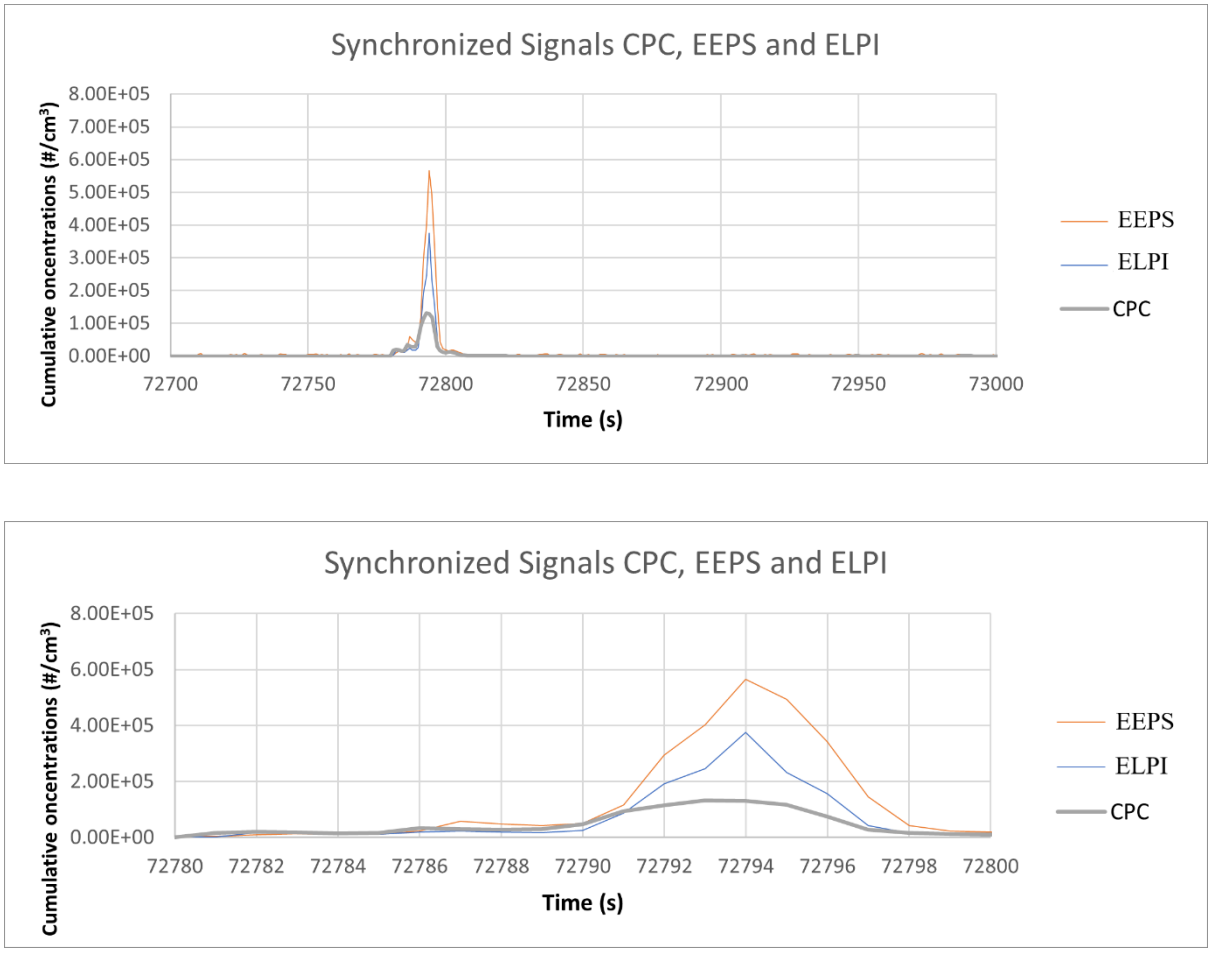

Figure 16. Synchronised Signal from the instruments

4.3 Detection Limit

The lowest possible concentration that the instrument can detect from the given concentration sample distinguishable from the noise. Detection limit specified by the manufacturers may not be the same always as it varies time and different operating conditions. The measuring instrument produces certain responses even without exposure to the sample known as background noise. These noises add up to the actual signal in real measurement which exaggerates the sample response [31]. The measuring location must also be taken into account, as differences will arise between samples measured in an open environment and those measured in a closed environment. Therefore, detection limit is setup considering 2 types of errors. Type 1 decision error (α) is also called false positive error which detects the concentration even though it is not present in the sample whereas false negative error called as type 2 error (β) which does not take the concentration response despite presence in the sample.

To determine the detection limit, it is recommended to consider the errors as low as possible and hence, the values of α and β were taken as 5% or 0.05. [32]

The detection limit is then obtained as a multiple of the standard deviation.

Limit of Detection (LOD) = 3.3 σ,

Where σ is the standard deviation of the instrument calculated from the background response. For the data set collected during the measurement, the standard deviation is taken from the signal recorded before the beginning of the first run. This takes into account only

the background concentrations and potential residual particles from previous runs which get resuspended with the incoming air flow from the follow up cycle start.

For the CPC, a standard deviation of 990.2 was obtained. Similarly, for the EEPS the standard deviation of the selected channels was calculated to be 32.02.

The time interval for estimating the standard deviation was 2000 s, with the background measured as the signal recorded before the start of the first run.

This gives us:

LOD_{CPC} =3267.6 #/cm^3

LOD_{EEPS} = 96.06 #/cm^3

4.4 Baseline and Peak

The response recorded by the instrument is a combination of both signal and noise and as a result there is uncertainty of the recorded response for the corresponding brake event. So, to reduce the measurement uncertainty the noise is minimized by subtracting the baseline value from total response of the event.

The procedure employed to create the baseline is by averaging the values for interval of 100 values just before and after the event and subtracting the baseline value from the Signal gives the useful signal. In the data obtained, the 10^{th} percentile was taken as the baseline to distinguish the useful signal from the background. The limit is set over the entire range of the

data set to get the value of the true response. This process is applicable to the data measured by the EEPS and the ELPI. The net concentration is obtained as:

$Concentration_{NET} = Concentration_{RECORDED} – Baseline,$

Where, $Concentration_{RECORDED}$ is the response recorded by the instrument.

4.5 Particle Size Distribution

Size of the particle is defined by its diameter known as particle diameter. Particles in a unit volume of sample can be classified into monodisperse and polydisperse depending upon their size ranges. Monodisperse particles have uniform size throughout and can only be produced under certain controlled laboratory conditions. On the other hand, polydisperse have particles with wide size ranges and the aerosol particles in the atmosphere are polydisperse in nature. Particles emitted from exhaust and non-exhaust sources are polydisperse in nature and its physical properties are strongly dependent on the size of the particle. Therefore, it is important to classify these size distributions by statistical means. For this, the entire size range is divided into series of successive size intervals and number of particles in each interval are determined. The size of each interval is called the bin width which varies with the instrument and its settings. Size bin is defined by the particle midpoint diameter (Dp) [33]

The particles emitted from brake fall into the category of polydisperse and therefore Particle Size Distribution is determined from particle number concentrations in respective size bins of

the measuring instrument. The concentration is plotted over the mid-point diameters (Dp) of the particles.

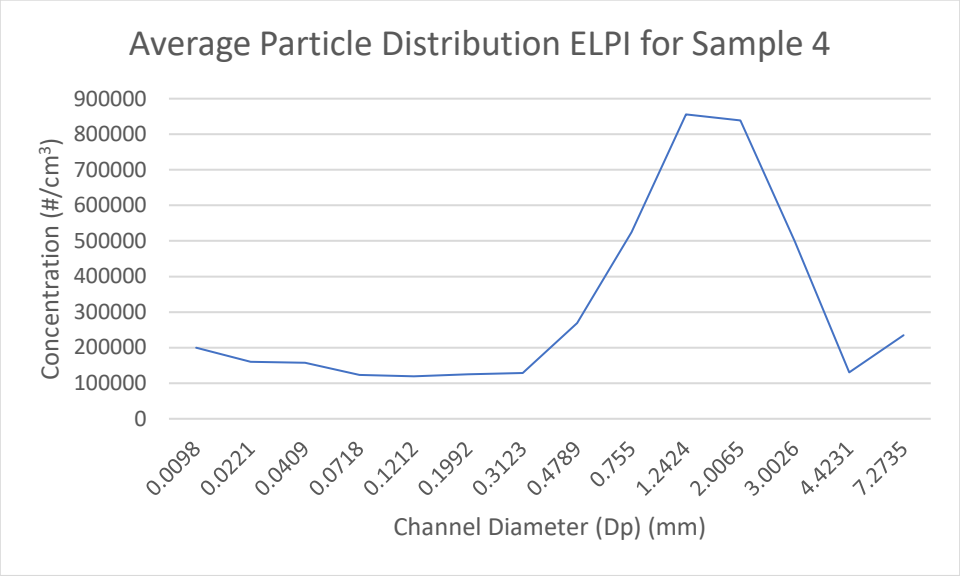

Figure 17. Particle Size Distribution of sample 4

The figure 17 shows the total particle size distribution of sample 4 measured over all the three runs from the ELPI data.

4.6 Brake Application

In order to better understand the generation of brake wear particles, the signal from the brake input is overlayed over the instrument reading of concentrations to identify any correlation between the brake input and wear particles generated. The Figure 18 shows how the brake signal has been overlayed over the signal from EEPS for sample 2.

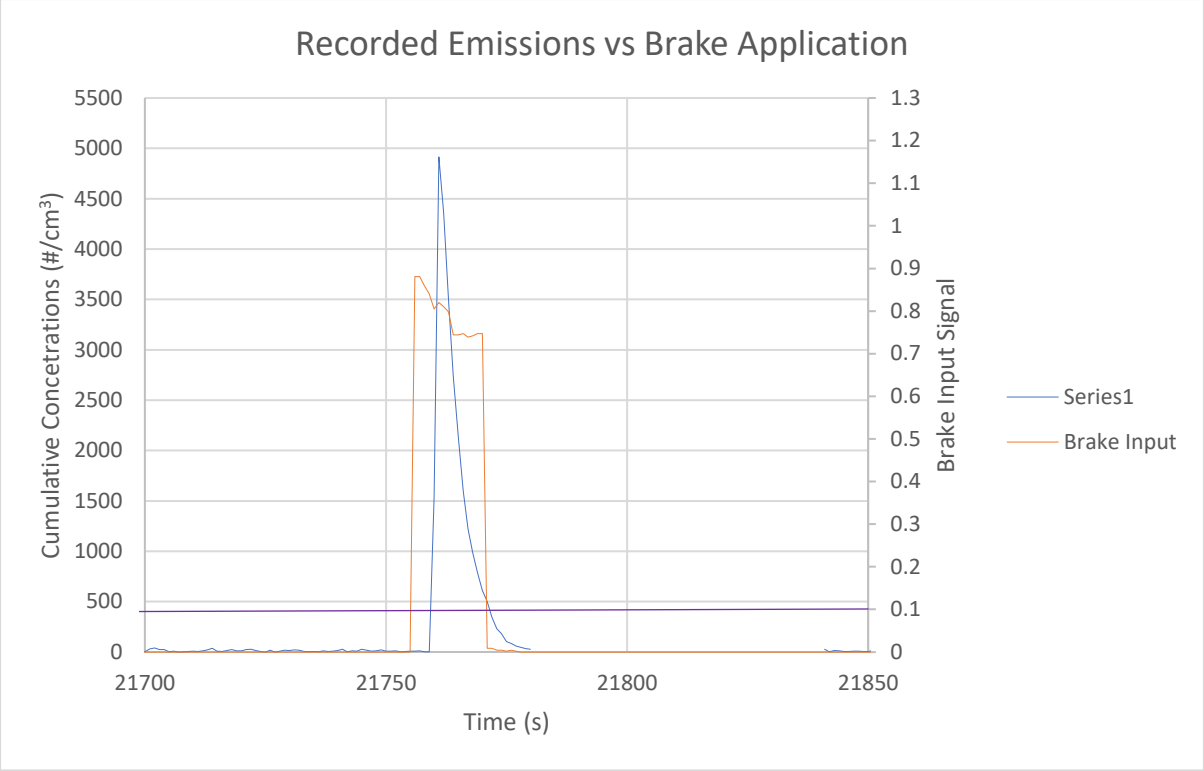

Figure 18. Cumulative Emissions and Brake Input Signal at a major braking event

The brake input – a voltage signal proportional to the hydraulic pressure in the brake calliper - is plotted against the right Y axis and is represented by the analogue signal obtained from the EEPS. The input signal over 0.1 (marked on the axis) is considered to be the baseline for the brake signal to account for any false positives and to identify the braking event in greater detail.

It is of interest to observe the emissions in a small interval before and after the application of the brakes. The particle concentrations at the highest braking events are discussed further.

5. RESULTS

5.1 Repeatability of data recorded.

Repeatability of an experiment is a measure of the likelihood of results produced from an experiment with the same setup and measuring instruments. To demonstrate the repeatability, the conditions of the experiment must be kept the same, which include:

- Location
- Measuring instruments
- Duration

In the tests conducted on the brake pads and disc, the conditions for the experiment were kept the same and the repeatability of the experiment on the different disc and pad materials was tested.

5.1.1 Repeatability of cumulative emissions

Sample 1

The Figures 19 and 20 show the cumulative concentrations recorded for Sample 1 from data collected by the CPC. Figure 19 shows the total cumulative concentrations over the course of the entire cycle, while Figure 20 shows the cumulative concentrations when the brakes are applied.

It is evident from the figures that there is no consistency between the third run, plotted against the right Y axis in the figures, and the remaining runs, with a large deviation from the

slopes of the other curves after ~6000s into the cycle. The concentrations then sharply increase with the final cumulative concentrations like that of run 2.

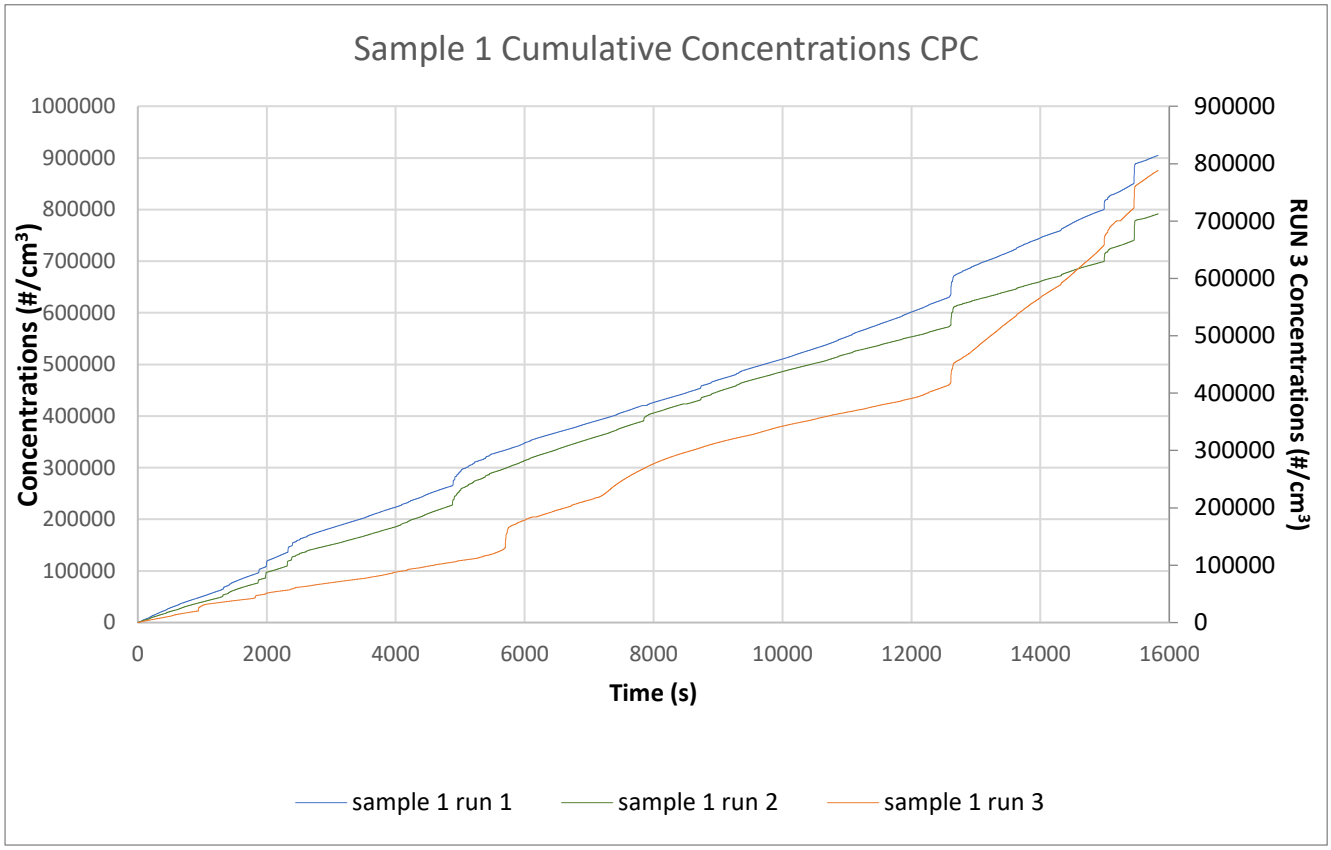

Figure 19. Cumulative CPC Concentration

When only braking events are taken into consideration the deviation of run 3 is seen in the same magnitude as that of the total cycle emissions. The curve for run 3 rises and follows the slope for run 2 towards the last few braking events and finally reports a final concentration figure lower than the other runs, thereby behaving expectedly with emissions reducing between consequent cycles.

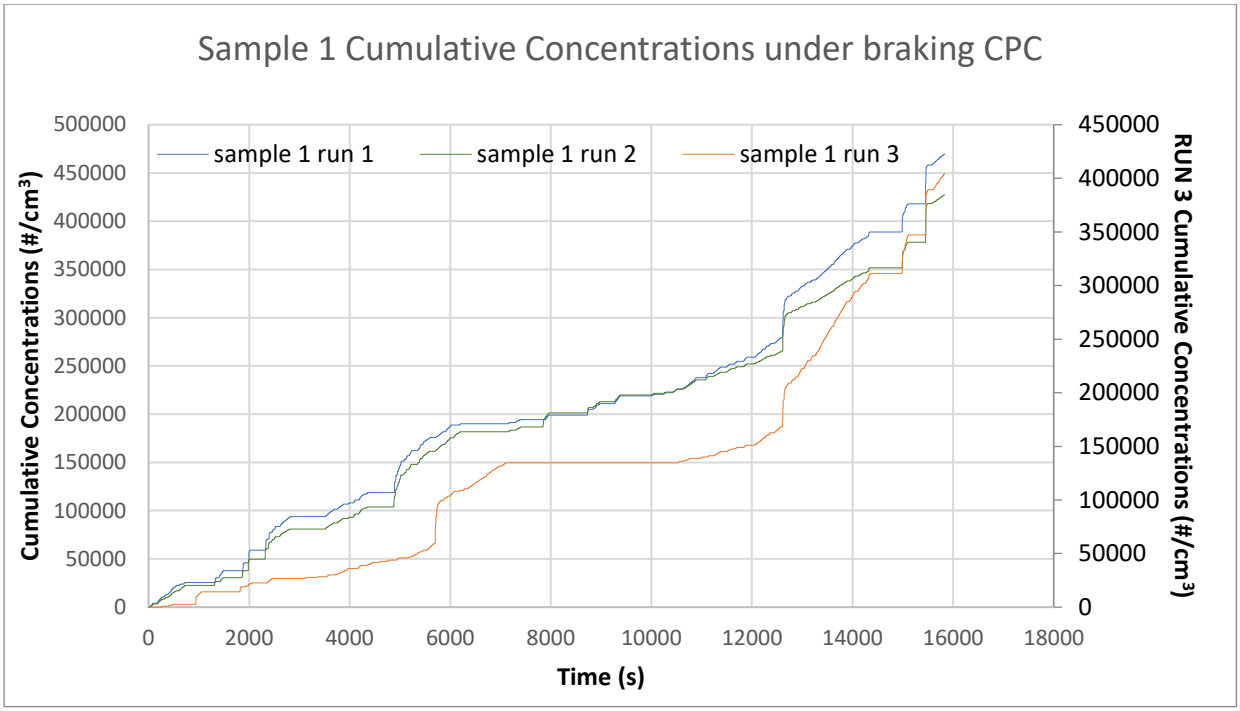

Figure 20. Cumulative Concentrations under braking measured by CPC

The Figures 21 and 22 here show the response of the EEPS, recording the cumulative concentrations over the total cycle (Figure 21) and when only considering the braking events (Figure 22).

From the graphs of the total cycle concentrations, we see that the concentrations reported during the third run, plotted against the right Y axis in the figures, are much higher as compared to the other two runs. This appears as an inconsistency with the behaviour observed in the other instruments for the same run. The accumulation pattern appears to be similar between all the runs with the difference lying in the magnitude of emissions in the case of run 3.

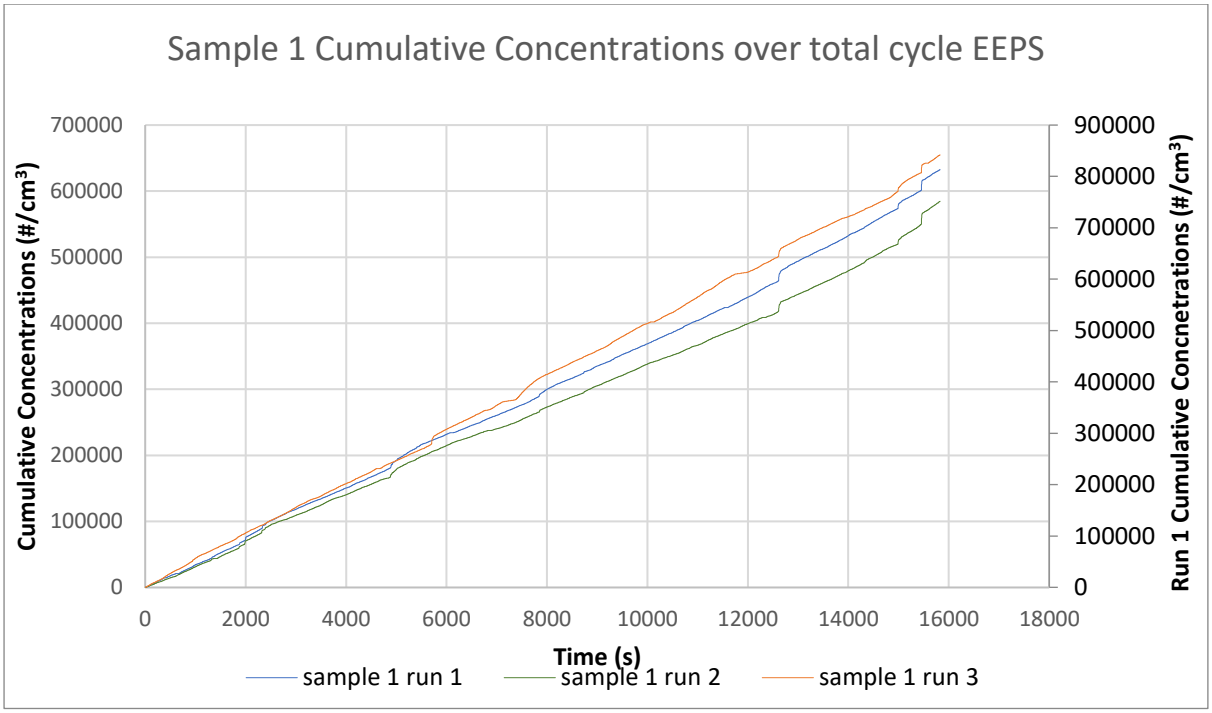

Figure 21. Cumulative Concentrations measured by EEPS

When only braking events are considered, seen here in Fig 22, the difference in the total PN reported by run 3 remains higher than the other runs but with a reduced margin. The moment of deviation from the other runs is also more clearly seen. Runs 1 and 2 appear to behave consistently and show a high degree of repeatability.

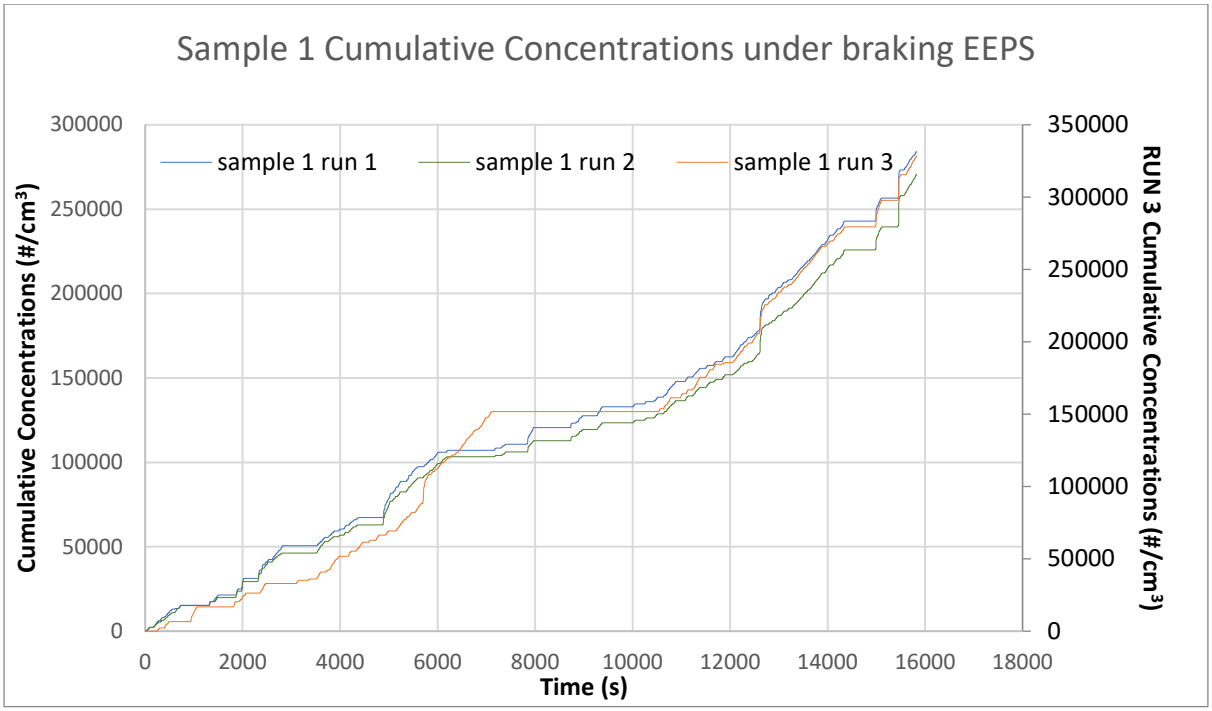

Figure 22. Cumulative Concentrations under braking measured by EEPS

The cumulative concentrations over the cycles as recorded by the ELPI are shown in the Figures 23 and 24. In the case of total cycle emissions, it is clearly seen that the runs 1 and 2 show extremely high degree of repeatability, with very marginal deviations. Run 3 shows inconsistency in the rate of cumulation but the curve follows the others for the last few braking events, recording lower concentrations than the other runs, which appears to contradict the behaviour reported by the EEPS.

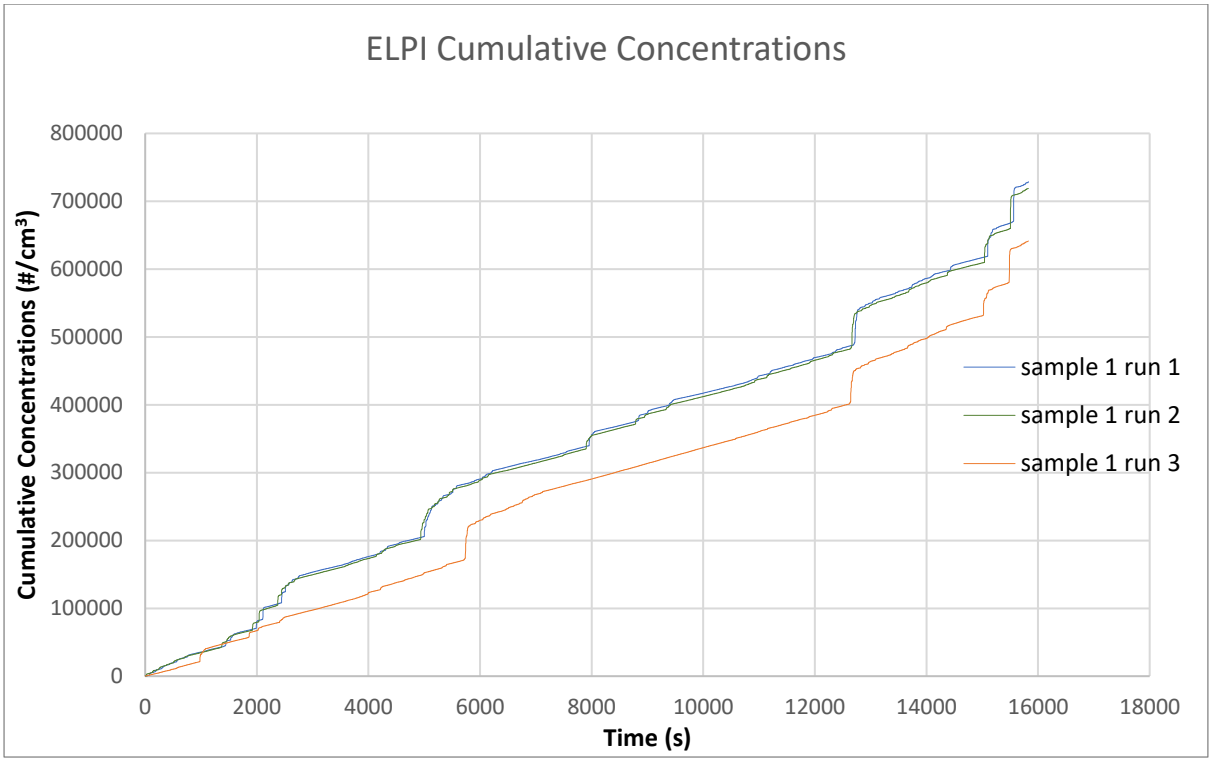

Figure 23. Cumulative Concentrations measured by ELPI

Runs 1 and 2 are again highly consistent with the cumulative concentrations reported under braking conditions only. The deviation of the third run can also be seen in the Figure 24, recording lower concentrations in the initial phase of the run but later following the other runs towards the end of the cycle.

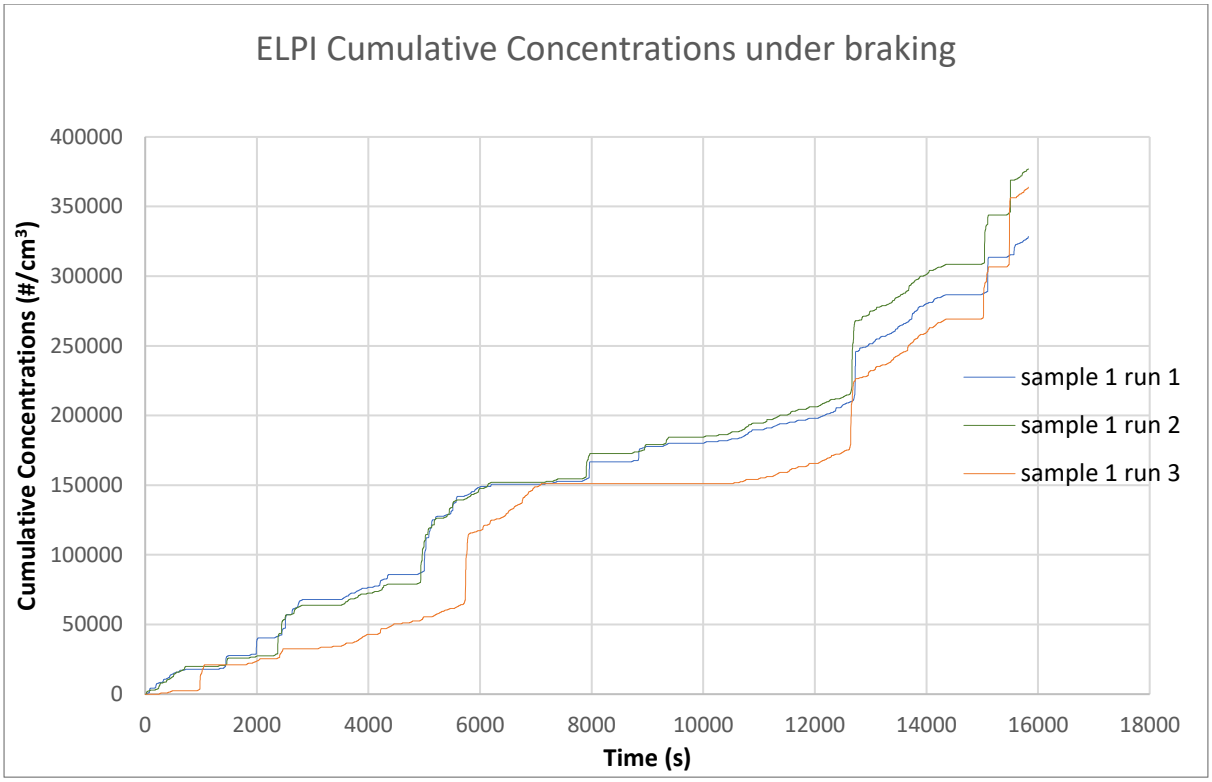

Figure 24. Cumulative Concentrations under braking measured by ELPI

The total cumulative concentrations during the whole cycle and only under braking conditions as measured by each instrument have been plotted in the Figure 25. The concentrations and the difference when considering only the braking events have been tabulated below.

Table 4. Total Cumulative Concentrations measured by CPC for whole cycle and only under braking

CPC	Cumulative Total PN (#/cm^3)	Total Cumulative PN Under braking (#/cm^3)	PN contribution of non-braking events (%)
RUN 1	904980	469445.1	48.1
RUN 2	791558	427215.3	46.0
RUN 3	788166	404190.1	48.7

Table 5. Total Cumulative Concentrations measured by EEPS for whole cycle and only under braking

EEPS	Total Cumulative PN (#/cm^3)	Total Cumulative PN Under Braking (#/cm^3)	PN contribution of non-braking events (%)
RUN 1	632426	284134	55.0
RUN 2	584562	270640	53.7
RUN 3	841723	328371	60.9

Table 6. Total Cumulative Concentrations measured by ELPI for whole cycle and only under braking

ELPI sample	Total Cumulative PN (#/cm^3)	Total Cumulative PN under braking (#/cm^3)	PN contribution of non-braking events (%)
RUN 1	728828	328568	54.9
RUN 2	718749	376863	47.5
RUN 3	641588	363860	43.2

The Tables 4-6 show the total cumulative PN concentrations measured by the instruments. A comparison has been made between the total PN during the cycle and when only braking events are considered.

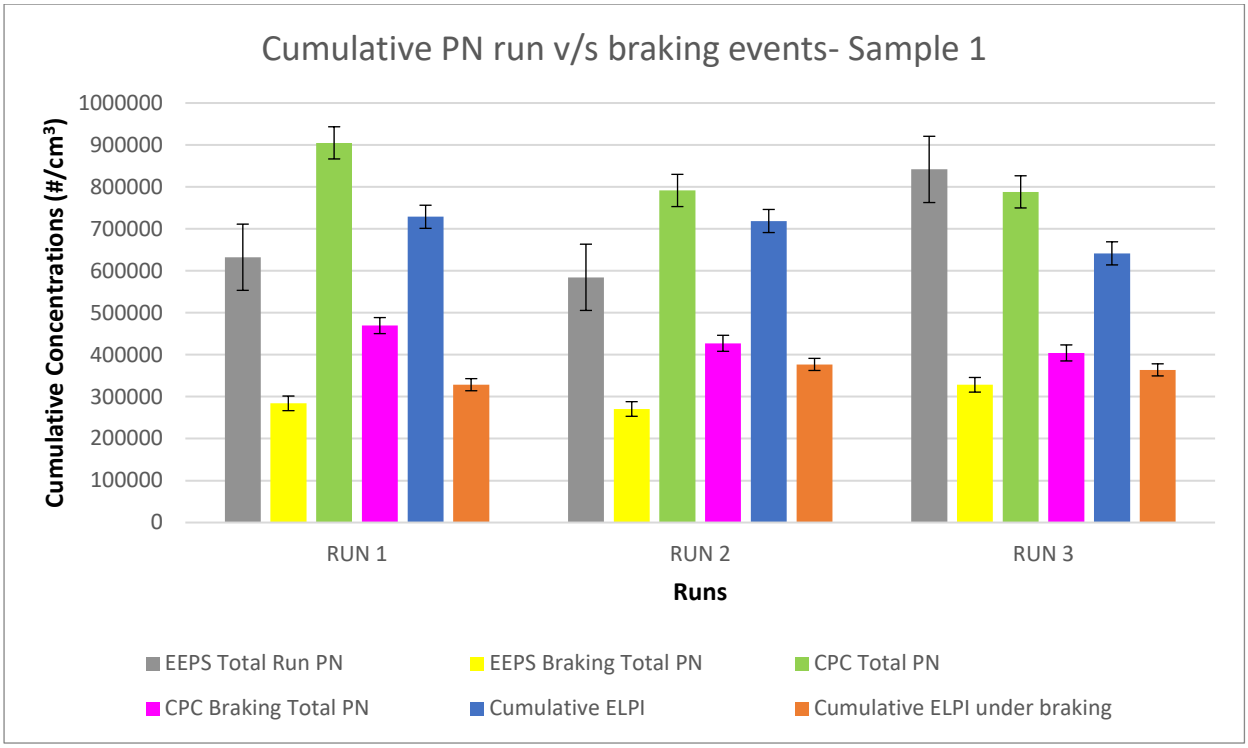

Figure 25. Comparison of cumulative concentrations over all runs and under braking

The Figure 25 compares the concentrations measured by the instruments over each run and over the braking events only for the sample 1.

Sample 2

Figures 26 and 27 below show the cumulative emissions from sample 2 recorded by the EEPS over individual runs (Figure 26) and over the braking events only (Figure 27).

The pattern of cumulation of the particles is repeatable to a high degree with a variation in magnitude for the first run. It is observed that the slopes of all the runs are the same with run 1 only differing from the other runs with fewer cumulative emissions.

When considering only the braking events in the runs, the degree of repeatability is higher than that for the case of emissions over the course of the entire run.

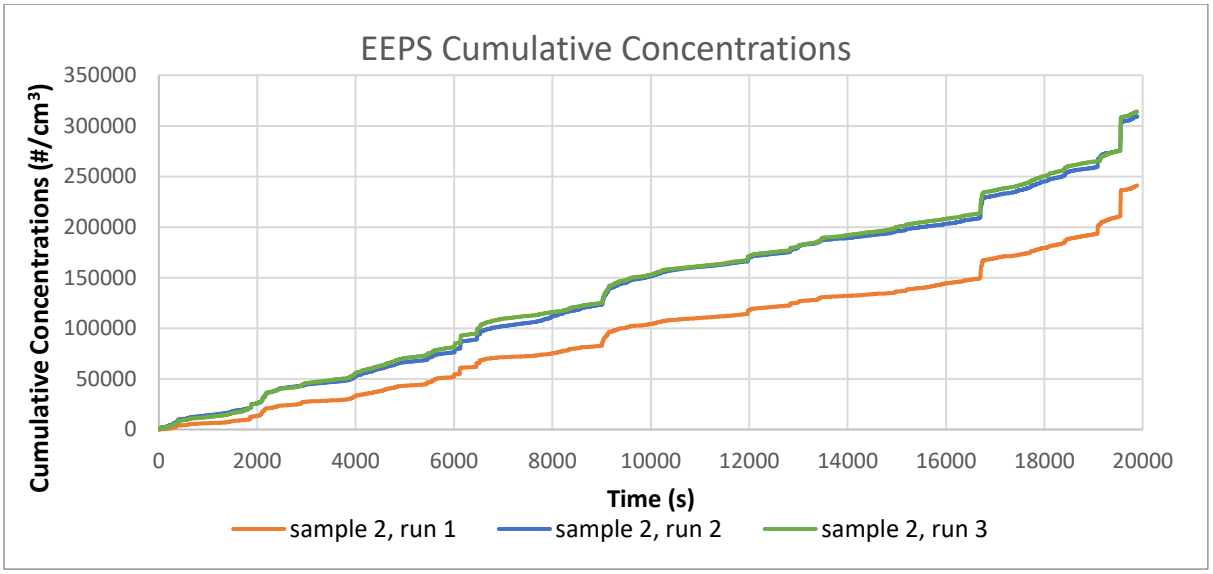

Figure 26. Cumulative Concentrations measured by EEPS

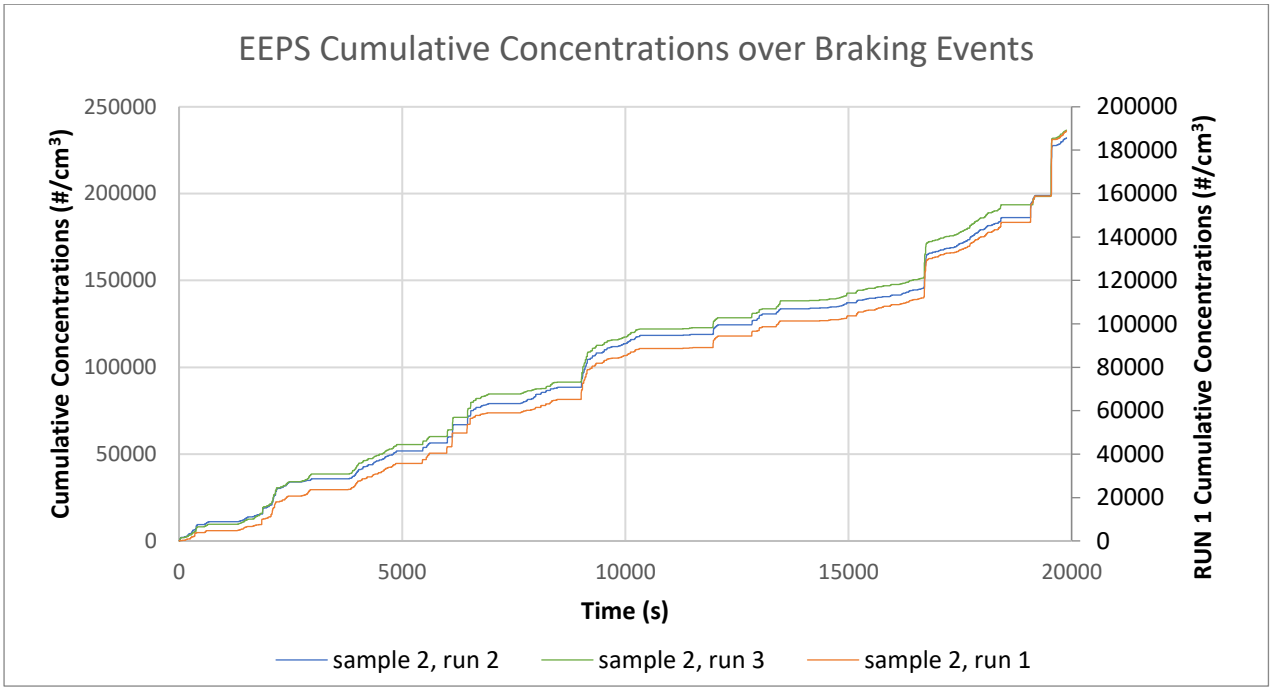

Figure 27. Cumulative Concentrations over braking events measured by EEPS

The Figures 28 and 29 below show the cumulative emissions from sample 2 as recorded by the CPC. Figure describes the pattern of accumulation of particles over the course of the individual runs whereas the figure shows the concentrations when brakes are applied during each run.

When compared with the EEPS curve, it is seen that the repeatability for the sample is not as consistent as in the case with the EEPS data, with Run 1 showing a high cumulation increase in the early part of the run. Following this point however, the curve reverts to a slope comparably similar to the other two runs.

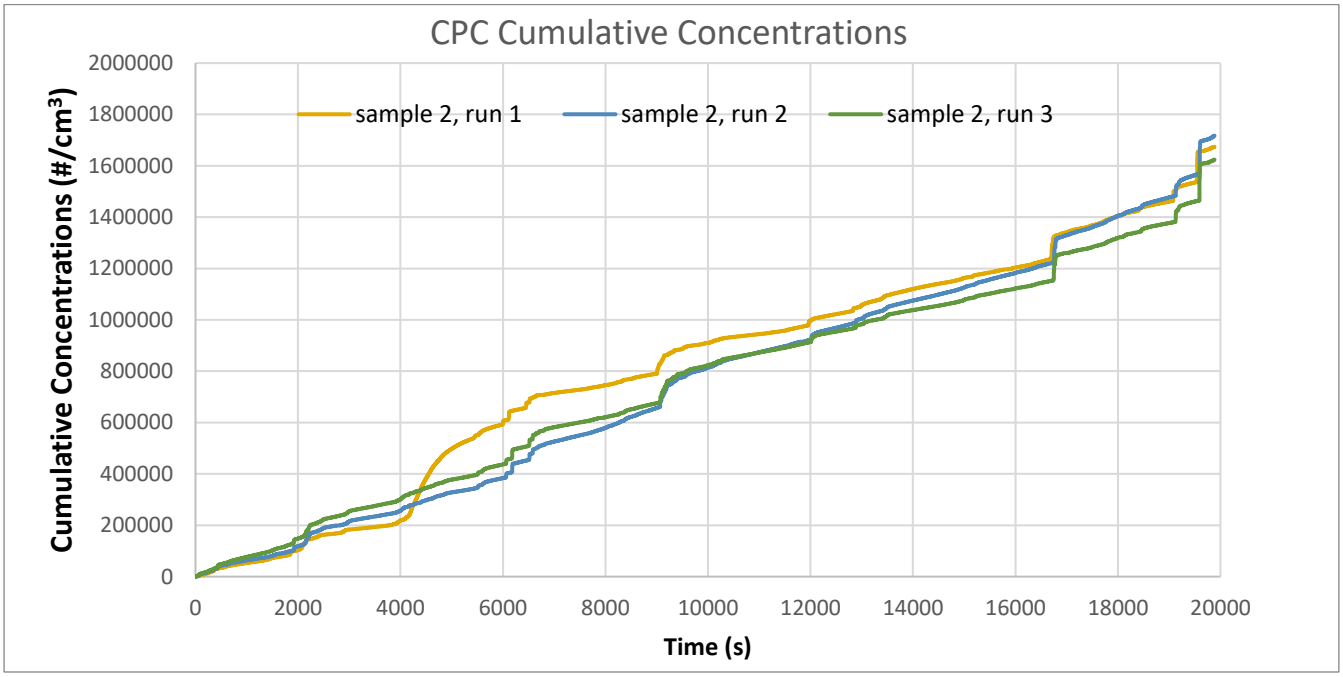

Figure 28. Cumulative Concentrations measured by CPC

When considering the cumulation with the application of brakes, the behaviour is similar to that of the whole run, with run 1 still exhibiting the increase in cumulative concentrations in the early part of the cycle and then matching the slope of the other two runs for the remaining part of the cycle.

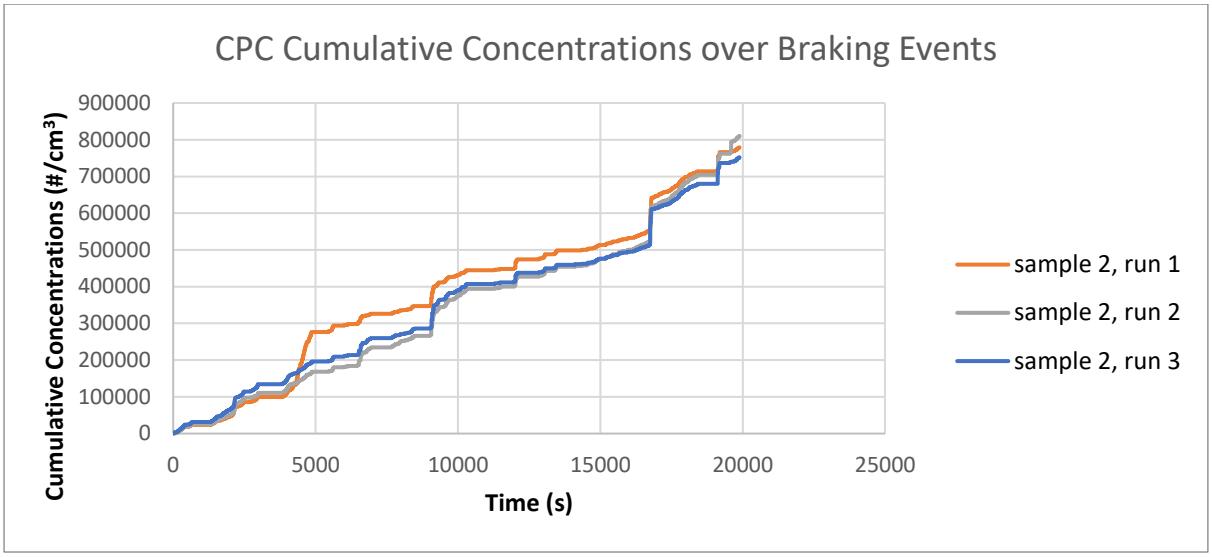

Figure 29. Cumulative Concentrations over only braking events measured by CPC

Figures 30 and 31 below show the cumulative concentrations of the sample 2 as recorded by the ELPI. The Figure 30 shows the concentrations over the course of each individual run. It is clearly seen that this sample exhibits very high degree of repeatability with marginal differences in the total cumulation.

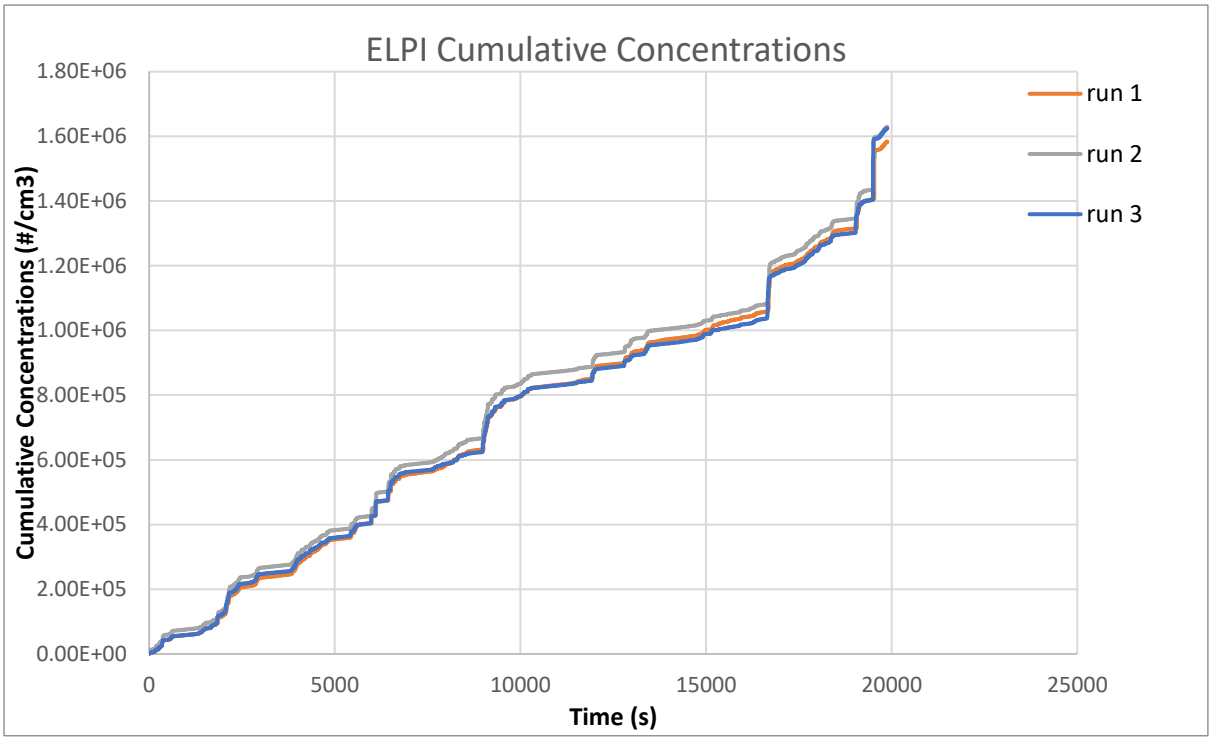

Figure 30. Cumulative Concentrations measured by ELPI

However, when the case of only braking events was considered, as shown in Figure 31 below, the repeatability over runs 2 and 3 remained unchanged. The cumulation curve of run 1 however shows a much larger value of particles cumulated during the run. Given that the curve development over the duration of the run is similar to that of the other two runs, it can be said that the cumulative data over the run 1 is offset by a constant multiple leading to the higher concentrations.

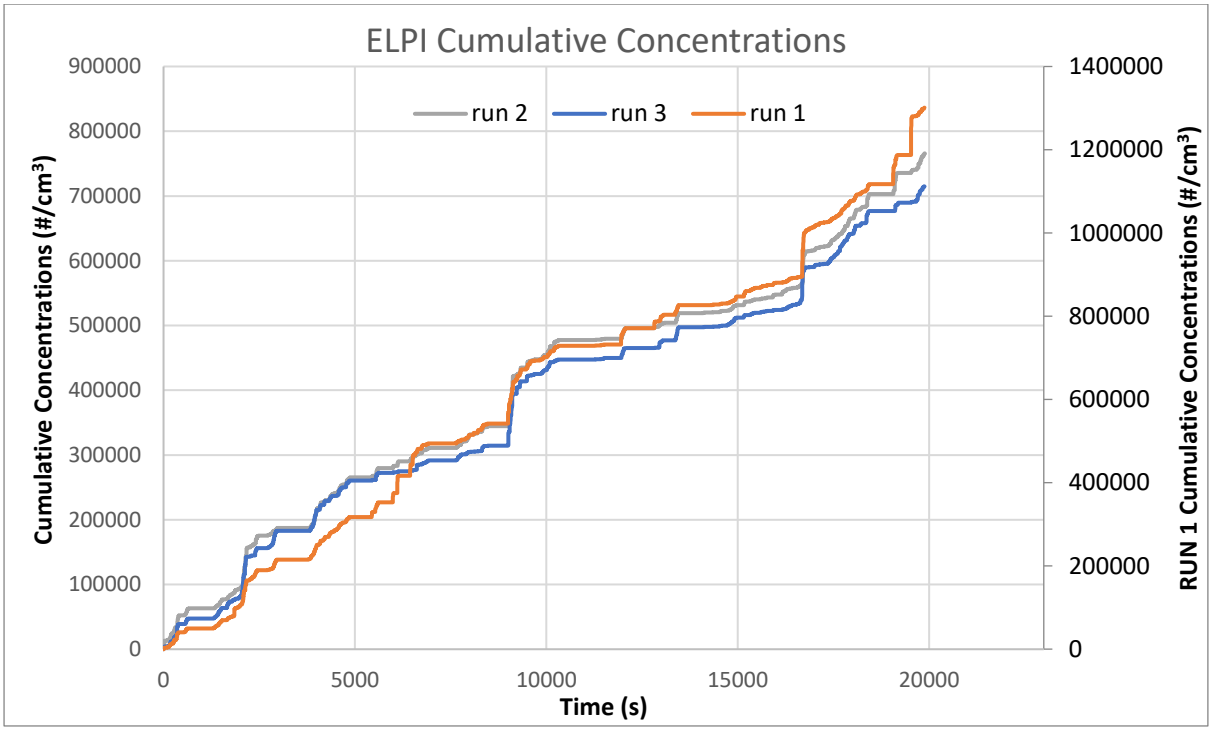

Figure 31. Cumulative Concentrations over braking events measured by ELPI

The total cumulative concentrations reported by the instruments for the cycle as well as under braking conditions have been tabulated below. The Figure 32 shows these concentrations plotted in comparison with each other.

Table 7. Total Cumulative Concentrations measured by CPC for whole cycle and only under braking

CPC	Total Cumulative PN (#/cm^3)	Total Cumulative PN under braking (#/cm^3)	PN contribution of non-braking events (%)
RUN 1	1674158	1120496	33.0
RUN 2	1719264	810504	52.8
RUN 3	1624501	752470	53.6

Table 8. Total Cumulative Concentrations measured by EEPS for whole cycle and only under braking

EEPS S2	Total Cumulative PN (#/cm^3)	Total Cumulative PN under braking (#/cm^3	PN contribution of non-braking events (%)
RUN 1	241063	188828	21.6
RUN 2	309490	232117	25.0
RUN 3	314218	236497	24.7

Table 9. Total Cumulative Concentrations measured by ELPI for whole cycle and only under braking

ELPI	Total Cumulative PN (#/cm^3)	Total Cumulative PN under braking (#/cm^3	PN contribution of non-braking events (%)
RUN 1	1583560	1301222	17.8
RUN 2	1629647	765718	53.0
RUN 3	1624365	714864	55.9

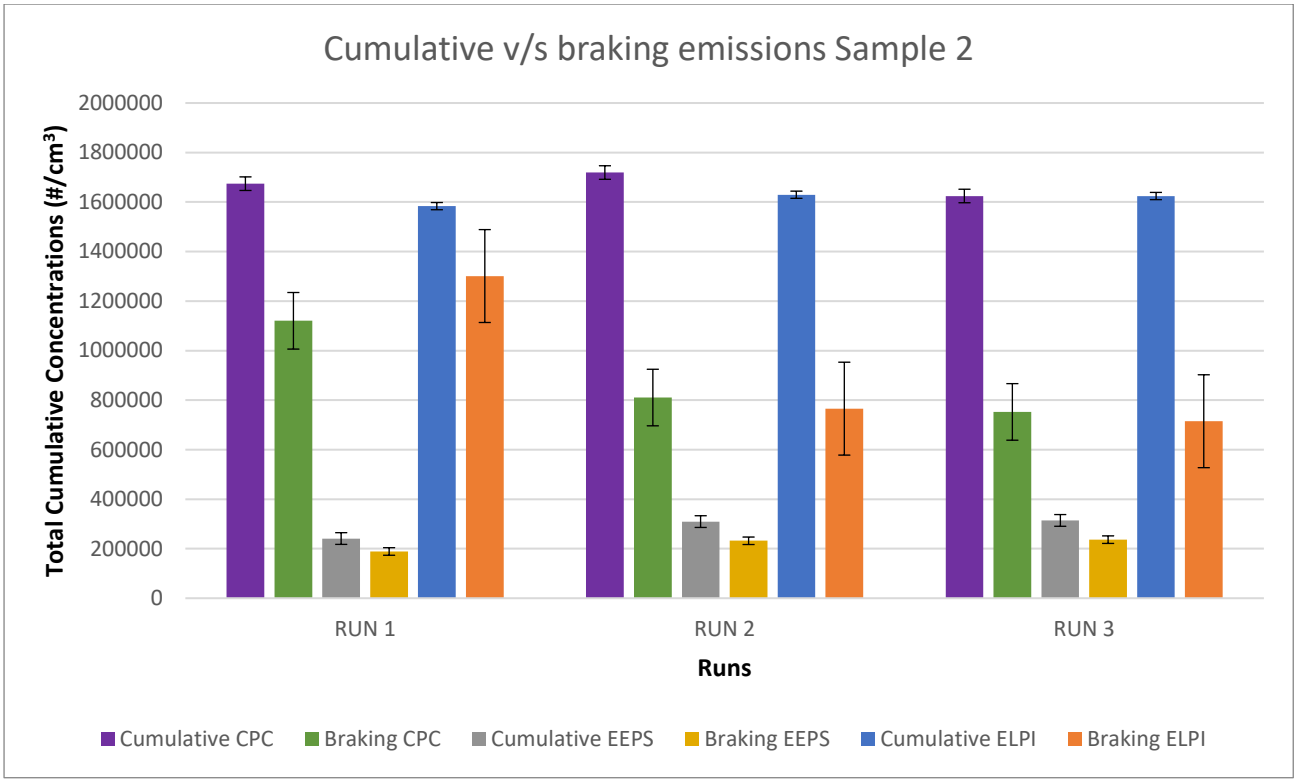

Figure 32. Comparison of cumulative concentrations over each run and cumulative braking emissions measured by all instruments

Sample 3

The cumulative emissions recorded by all the instruments for the sample 3 were plotted against the time elapsed during the cycle and compared with each run.

The Figures 33 and 34 below show the cumulative emissions from individual runs accumulated over the course of the entire run. It is clearly seen that runs 2 and 3 are remarkably similar in progression and exhibit a similar slope to that of run 1. The first run, while a little similar to the other runs in terms of curve profile, reports a concentration value higher than that of the other runs.

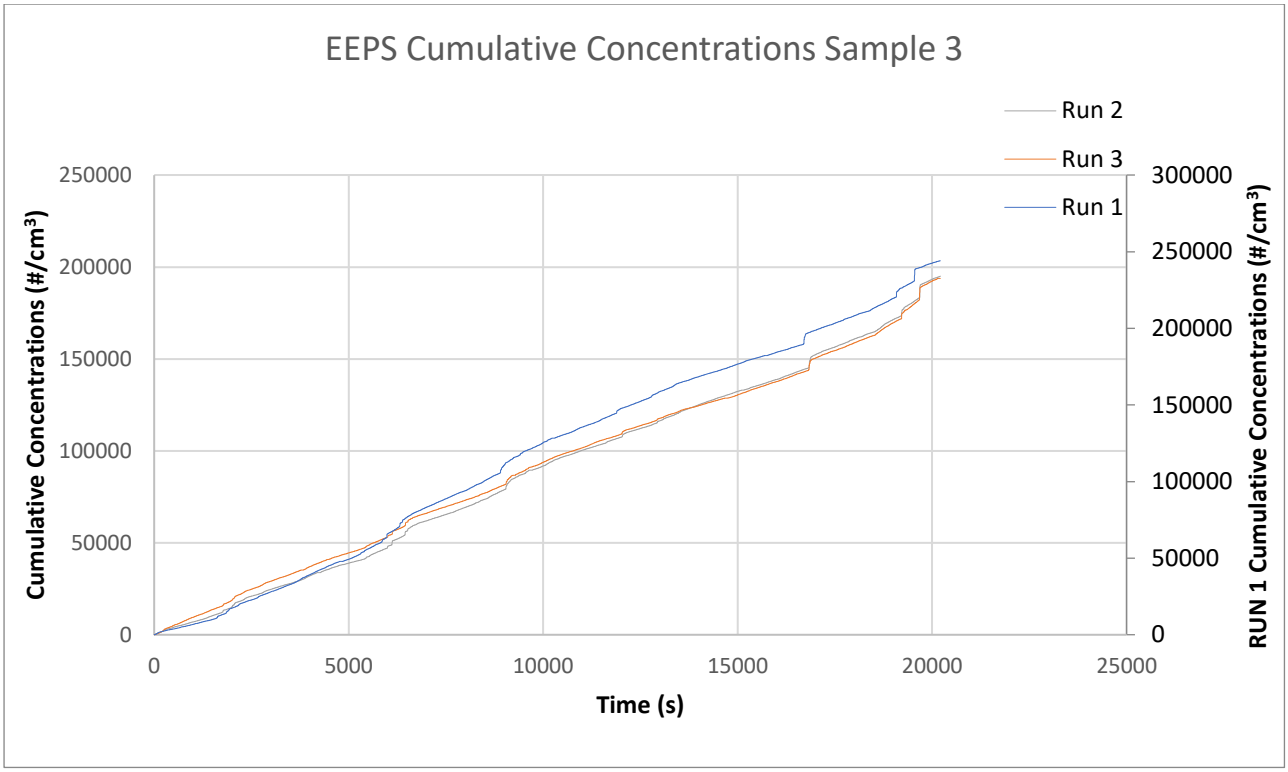

Figure 33. Cumulative Concentrations measured by EEPS

When the braking events are considered (shown in Figure 34), the offset between the first run and the others is more clearly seen. As with the previous case, the progression of cumulation of emissions is similar for all the runs and the primary deviation between the runs is the offset.

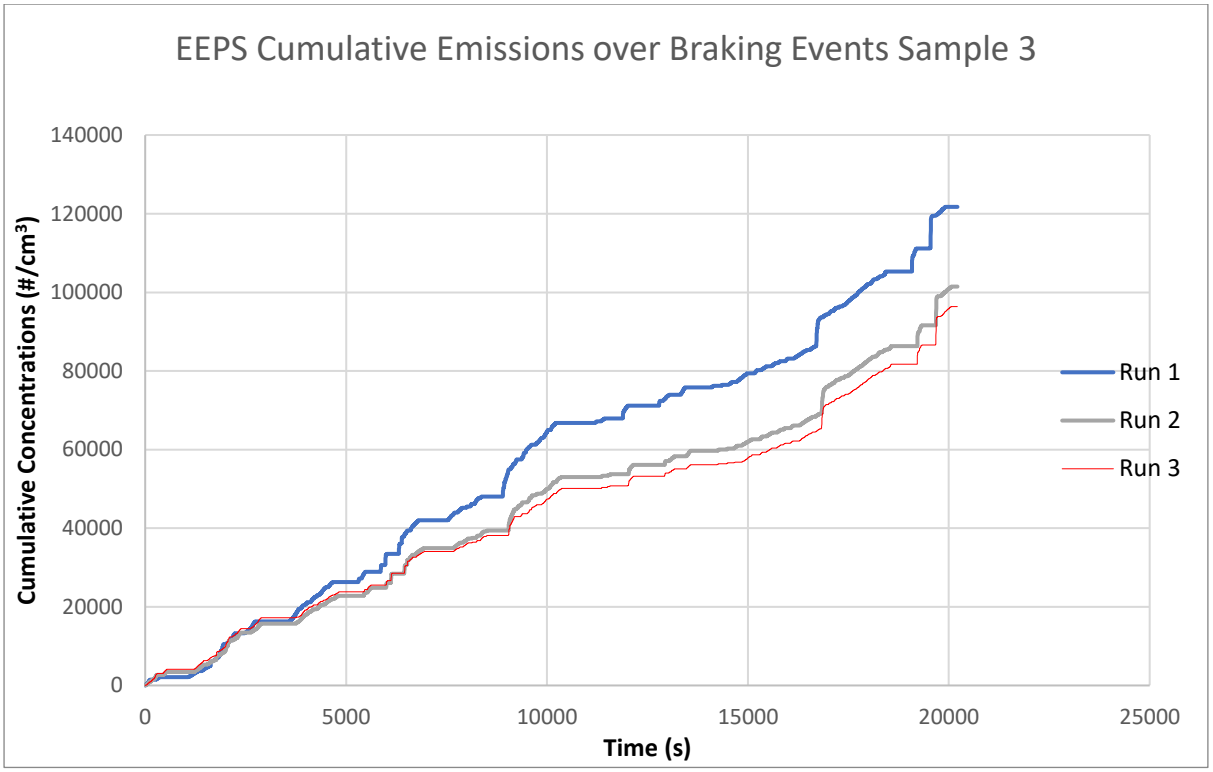

Figure 34. Cumulative Concentrations over braking events measured by EEPS

Figures 35 and 36 show the cumulative concentrations during each run of the WLTP cycle for the sample 3 as recorded by the ELPI and when only the braking events of those runs are considered.

The emissions over the course of each run shows considerable variation in the summation of concentrations recorded, with each run offset from the other by a small margin. The shape of the curves for all the runs however are similar, with a difference of ~20% higher for run 1, and exhibit a good degree of repeatability under the conditions of the experiment.

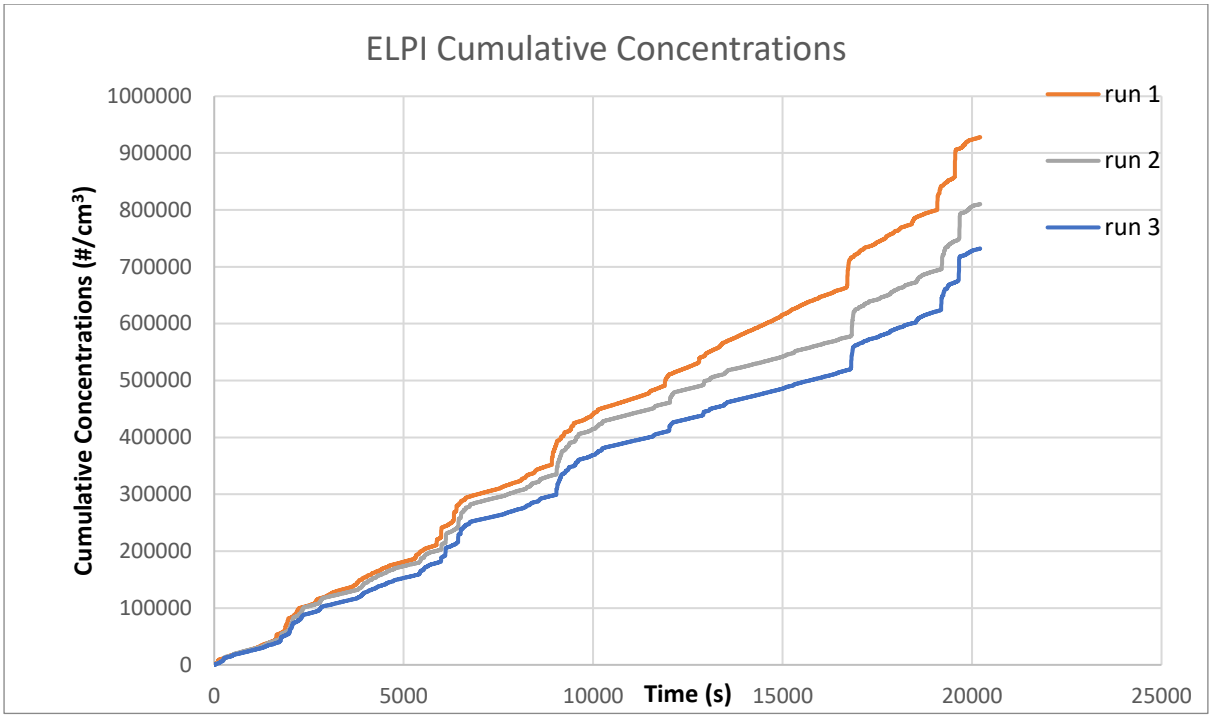

Figure 35. Cumulative Concentrations measured by ELPI

When the cumulative emissions considering only the braking events of each run are compared, the difference in total cumulative concentrations of run 3 are reported to be significantly lower as compared to the other two runs, which means that the share of non-braking events is ~57% more than that of the braking events. The share of non-braking events in the other two runs was calculated at 33.7% and 30% respectively. The general pattern of the cumulative concentrations reducing after successive runs is also observed.

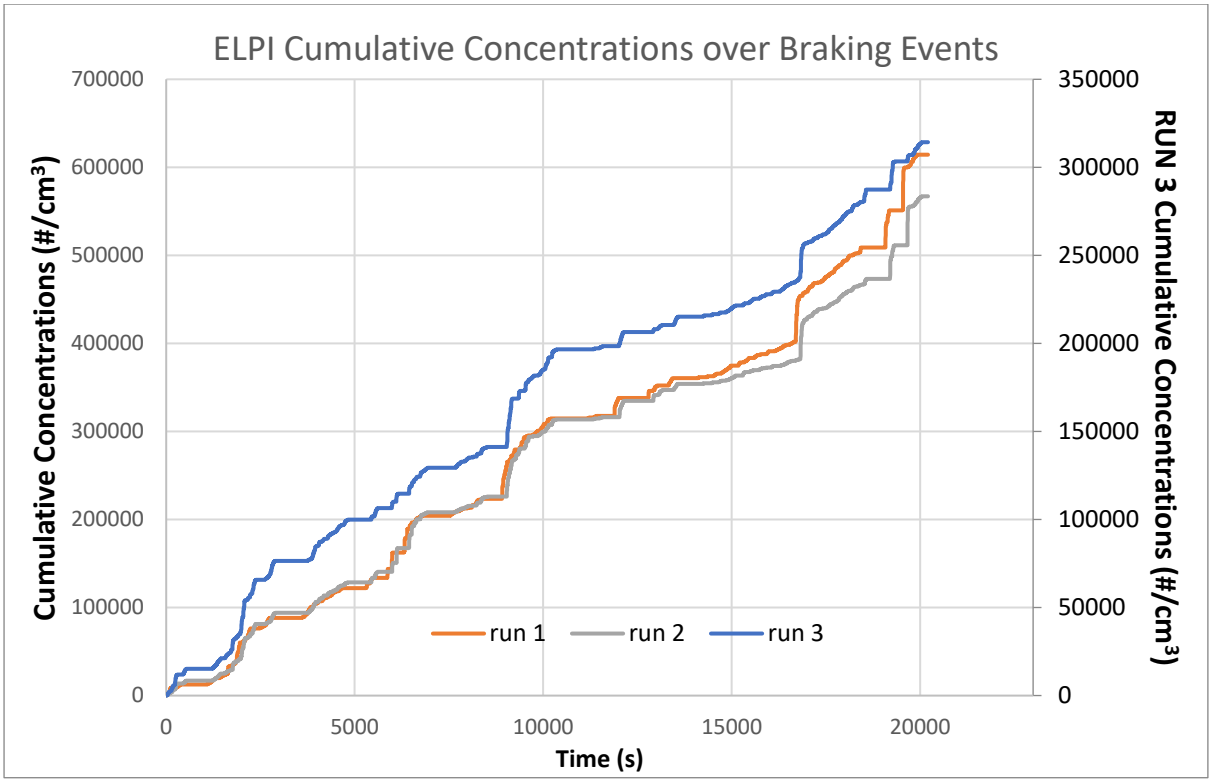

Figure 36. Cumulative Concentrations over braking events measured by ELPI

The Figure 37 below shows the cumulative concentrations recorded by the CPC over each run. It was observed that for this sample there is significant variation in the emissions accumulated during the runs even though the pattern of accumulation remains very similar to the other cycles, with all increments in the concentration levels being of the same magnitude.

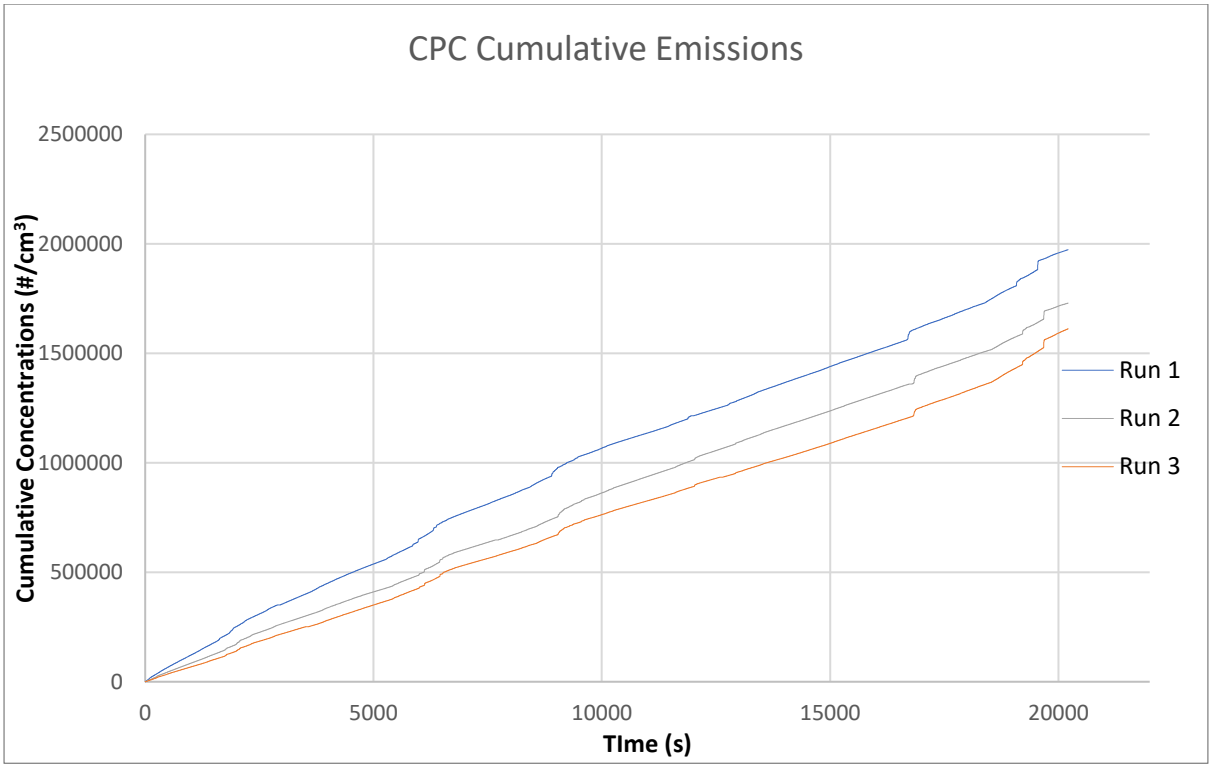

Figure 37. Cumulative Concentrations measured by CPC

The Figure 38 shows the data from CPC for Sample 3 when only the braking events in the run are considered. Here we see that there is not much change in the difference of cumulated values and the slopes of individual runs. It can be deduced that the repeatability of the experiment is good but the variation in reported numbers is a result of an offset in the data recorded.

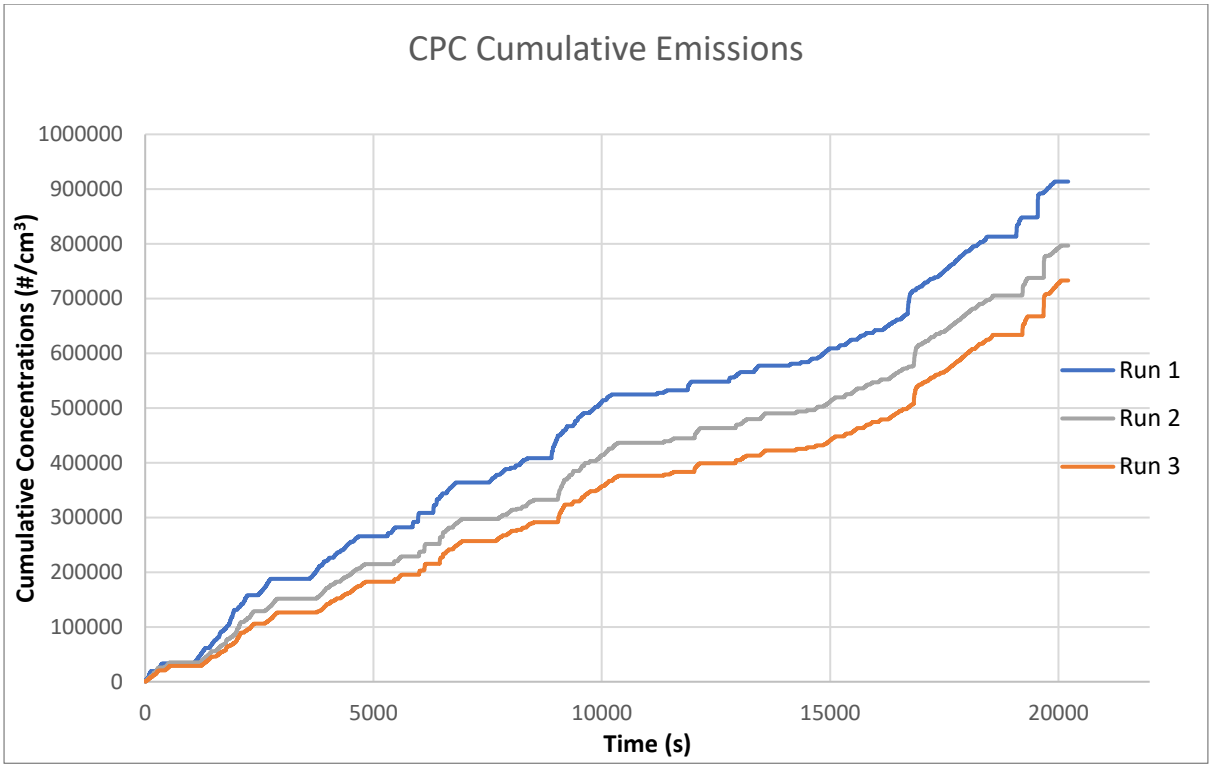

Figure 38. Cumulative Concentrations over braking events measured by CPC

To compare the instrument responses for the sample, the total cumulative concentrations for the duration of the entire cycle as well as only under braking are plotted and tabulated below.

The Figure 39 shows the differences in the magnitude of instrument responses in each run of the WLTP Brake cycle.

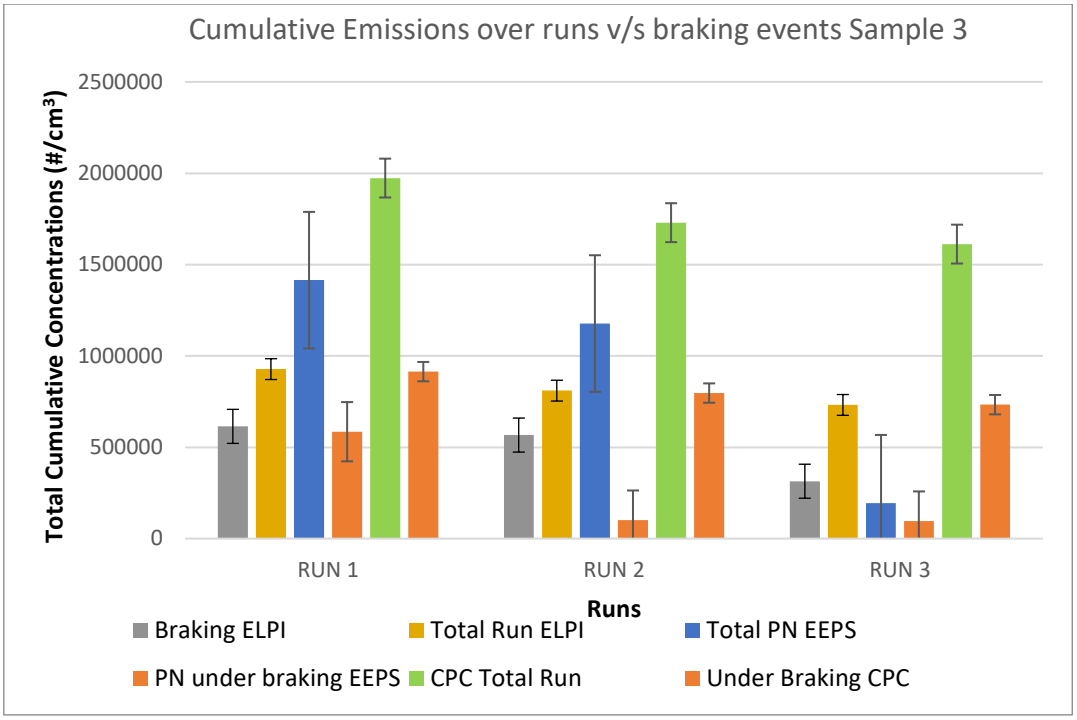

Figure 39. Comparison of cumulative and cumulative braking emissions of Sample 3

Table 10. Total Cumulative Concentrations measured by CPC for whole cycle and only under braking

CPC	Total Cumulative PN (#/cm³)	Total Cumulative PN under braking (#/cm³)	PN contribution of non-braking events (%)
RUN 1	1973642	914106	53.6
RUN 2	1729600	796809	53.9
RUN 3	1612229	733228	54.5

Table 11. Total Cumulative Concentrations measured by ELPI for whole cycle and only under braking

ELPI	Total Cumulative PN (#/cm³)	Total Cumulative PN under braking (#/cm³)	PN contribution of non-braking events (%)
RUN 1	927868	614434	33.7
RUN 2	810185	567052	30.0
RUN 3	731945	314245	57.0

Table 12. Total Cumulative Concentrations measured by EEPS for whole cycle and only under braking

EEPS	Total Cumulative PN (#/cm^3)	Total Cumulative PN under braking (#/cm^3)	PN contribution of non-braking events (%)
RUN 1	1414864	585292	58.63
RUN 2	1177456	101466	91.38
RUN 3	193887	96364	50.30

Sample 4

The cumulative emissions recorded by each of the instruments (CPC, EEPS and ELPI) were segmented for each of the test runs, and further to include the particle concentration measured only during the braking events. The data from each run is then plotted and compared.

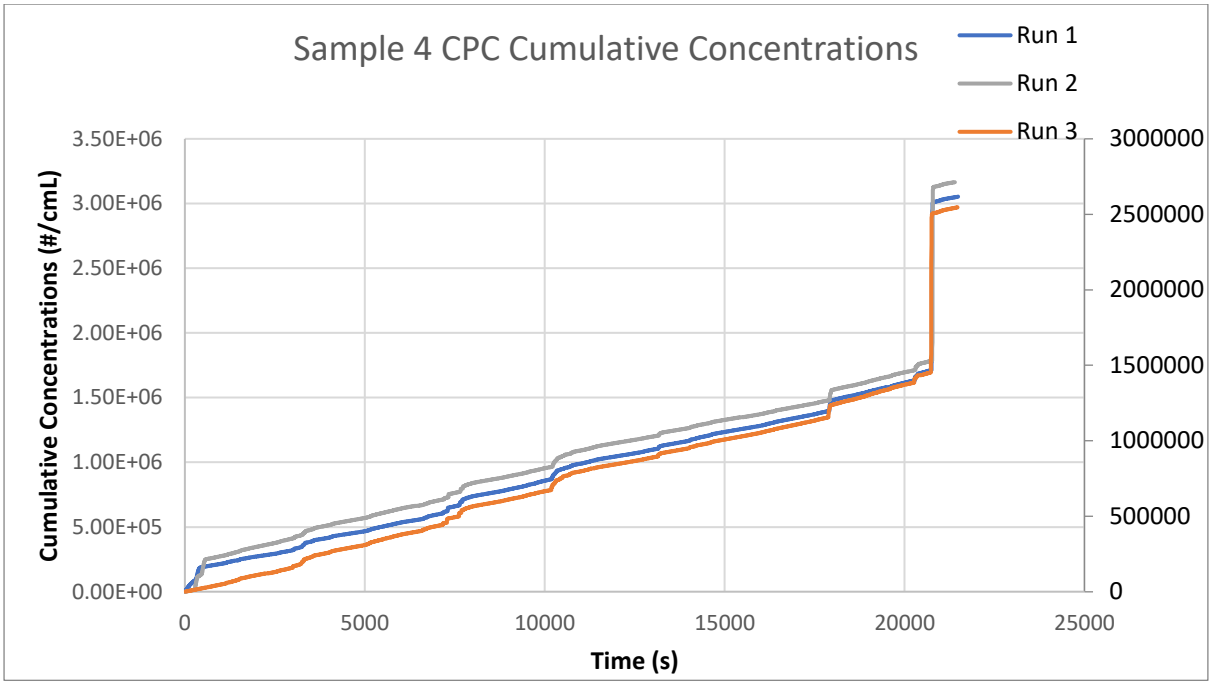

Figure 40. Cumulative Concentrations measured by CPC

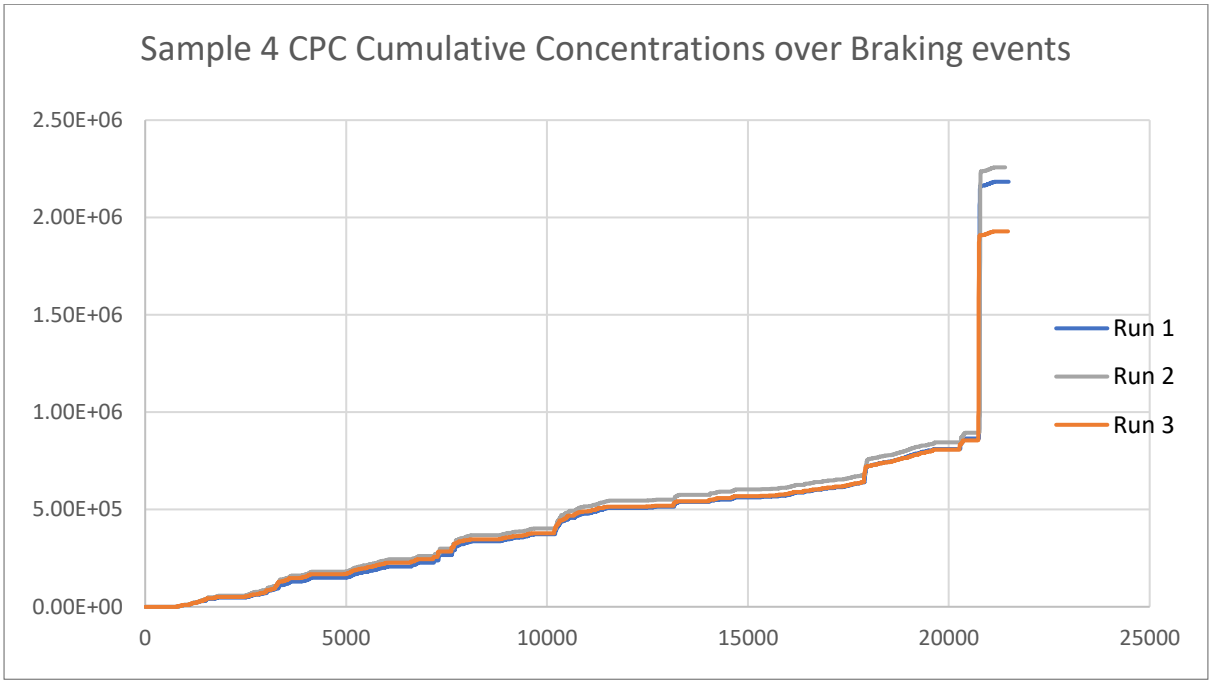

Figure 41. Cumulative Concentrations over braking events measured by CPC

The Figures 40 and 41 show the comparison between the 3 runs of the WLTP cycle on Sample 4 as recorded by the CPC. Figure 40 is the cumulative emissions over the entire run and Figure 41 shows the cumulative emissions from the braking events.

The figures show a very high degree of repeatability in the response from the CPC. In the emissions over the entire runs, the slopes for each of the runs are very similar, with runs 1 and 2 reporting similar concentration numbers. The deviation of run 3 from the other runs is a possible result of an offset in the data as the slope of the curve is the same while the reported numbers are higher by a small multiple.

When the emissions from the braking events are considered, the repeatability is comparatively higher than that over the entire run. The offset seen in the data for run 3 is not observed when the braking pressure is applied leading to the possibilities that the offset caused in Figure 40 is in the background or a consequence of resuspended particles well after the brakes are fully released during the third run. Table 14 lists the cumulative concentrations for the complete run and emissions under braking conditions only. The share of non-braking events to the total PN concentrations is then calculated from the difference in the two tabulated concentrations.

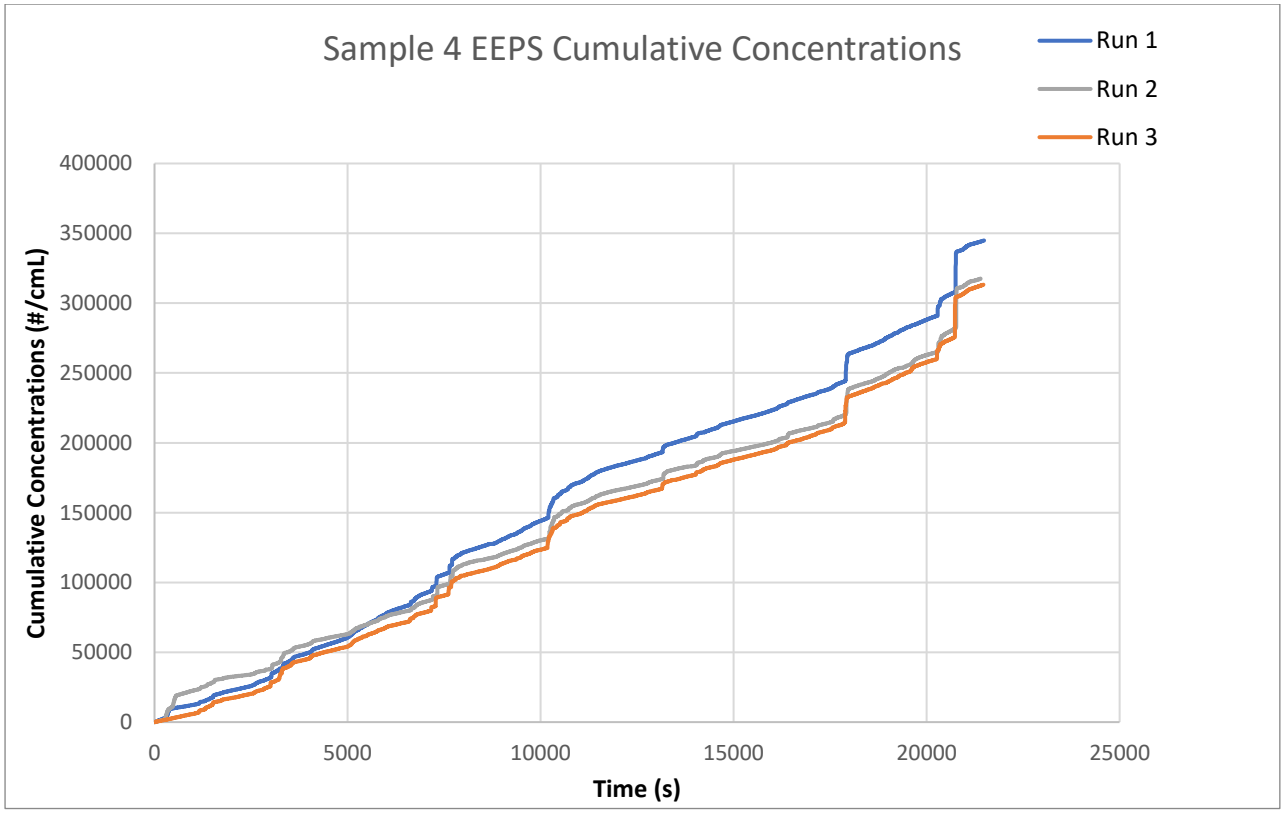

Figure 42. Cumulative Concentrations measured by EEPS

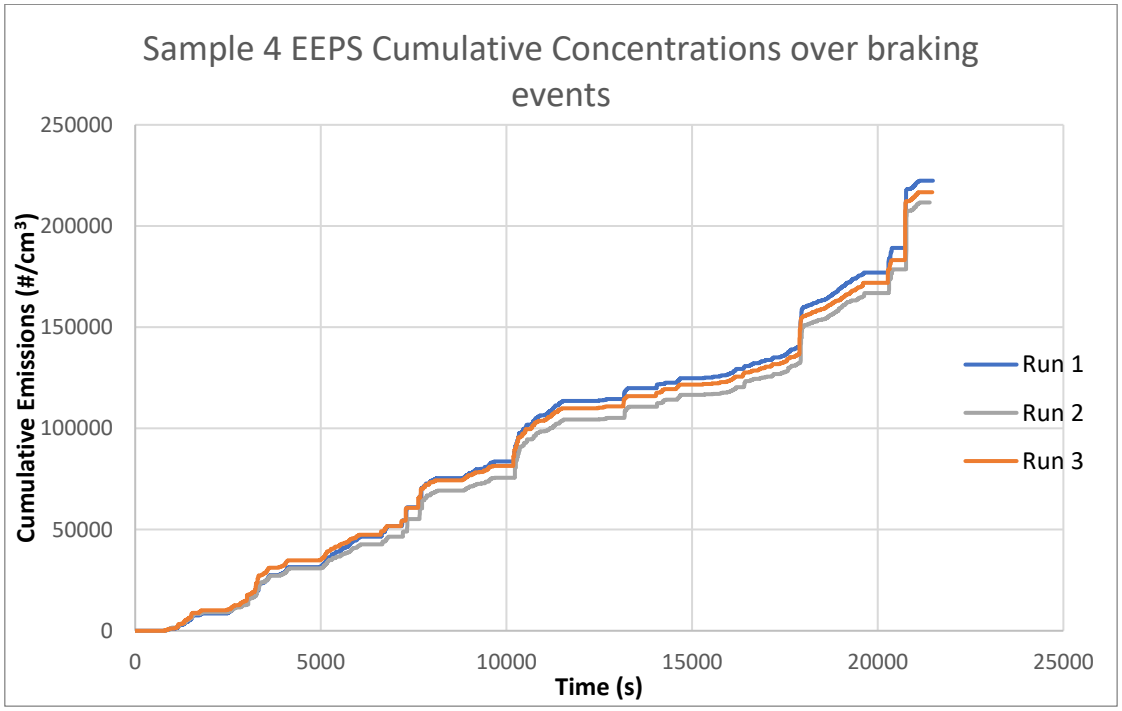

Figure 43. Cumulative Concentrations over braking events measured by EEPS

The Figures 42 and 43 show the cumulative responses recorded by the EEPS for Sample 4 over the course of 3 runs of the WLTP cycle. Figure 42 is the recorded cumulative emissions over the entire run, while Figure 43 shows the cumulative emissions from the braking events in each of the runs. The share of total cumulative emissions and the emissions from braking events only have been compared in Table 15.

As with the data from the CPC, the runs recorded by the EEPS also show a high degree of repeatability of the individual runs as the slopes of the runs are significantly close to each other. Run 1 reports a higher cumulative concentrations, but as in the case of the CPC data, the deviation is a result of an offset of the data accumulated in run 1, with the pattern of accumulation over the run being similar to those of the other runs.

In Figure 43, where only the braking events in the cycle are reported, there is no offset and the runs show a very high degree of repeatability once again.

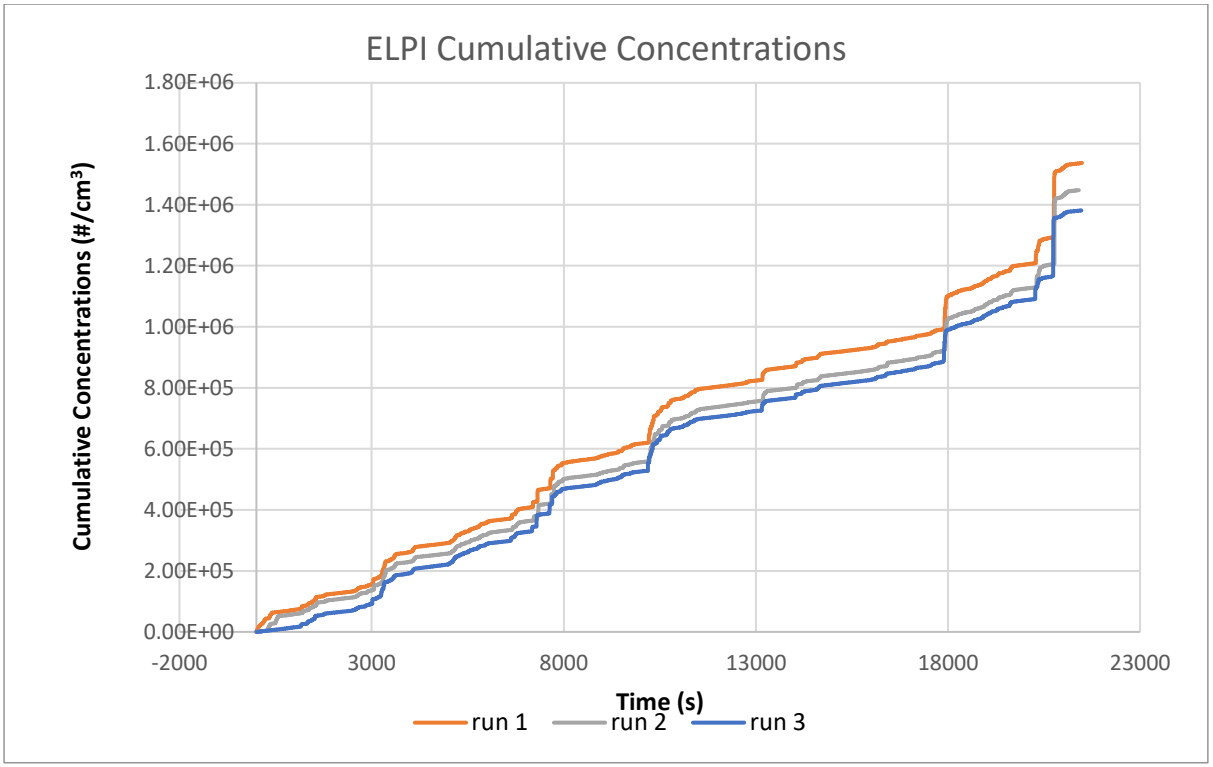

Figure 44. Cumulative Concentrations measured by ELPI

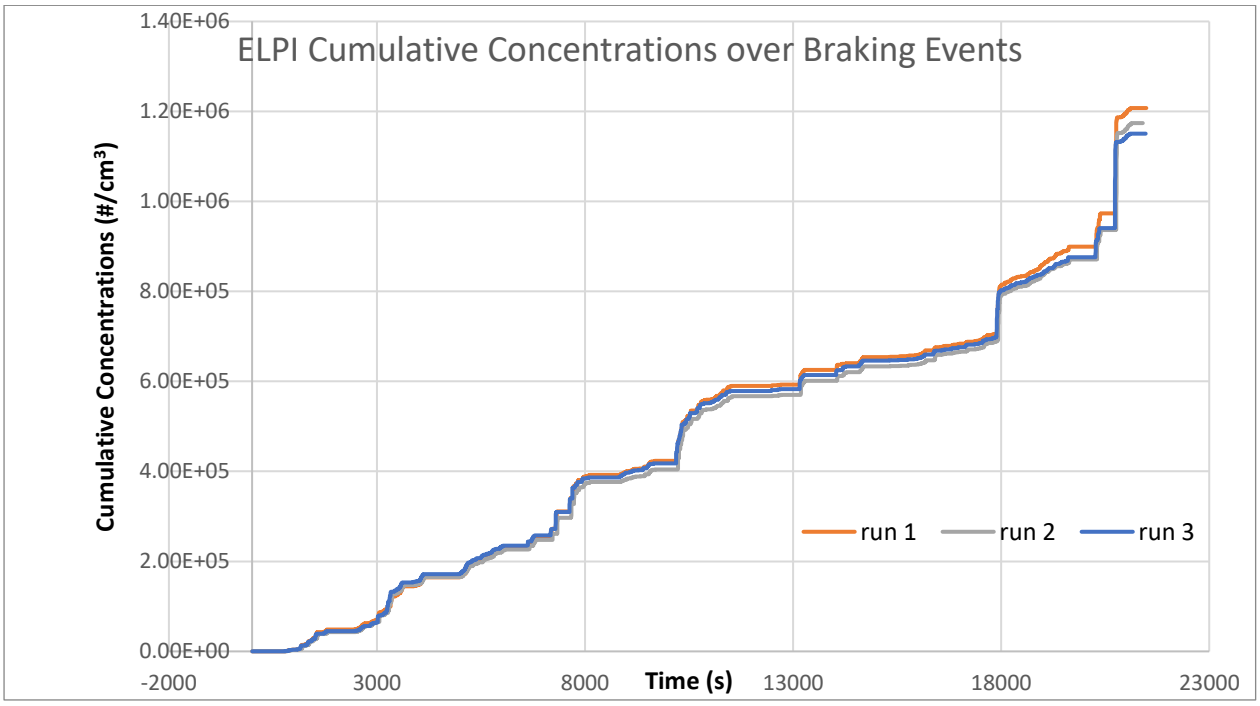

Figure 45. Cumulative Concentrations over braking events measured by ELPI

Figures 44 and 45 show the cumulative emissions recorded by the ELPI and accumulated over the entire individual run (Figure 44) and with only the braking events in each run considered (Figure 45).

Addressing the repeatability of each run, the response recorded by the ELPI exhibits

It is also seen that the numbers reported by the CPC and EEPS are of the same range, the ELPI reports significantly higher concentrations. The ultra-fine particles from brake wear tend to accumulate together to form particles of diameters in the micro-meter range. Due to this accumulation, it is possible that the ELPI, which has the capability of measuring particles with larger diameters, detects these larger particles which avoid detection by the EEPS.

Figure 46 compares the cumulative concentration measured by the instruments for each run. Also compared in the figure are the cumulative concentration from the braking events only.

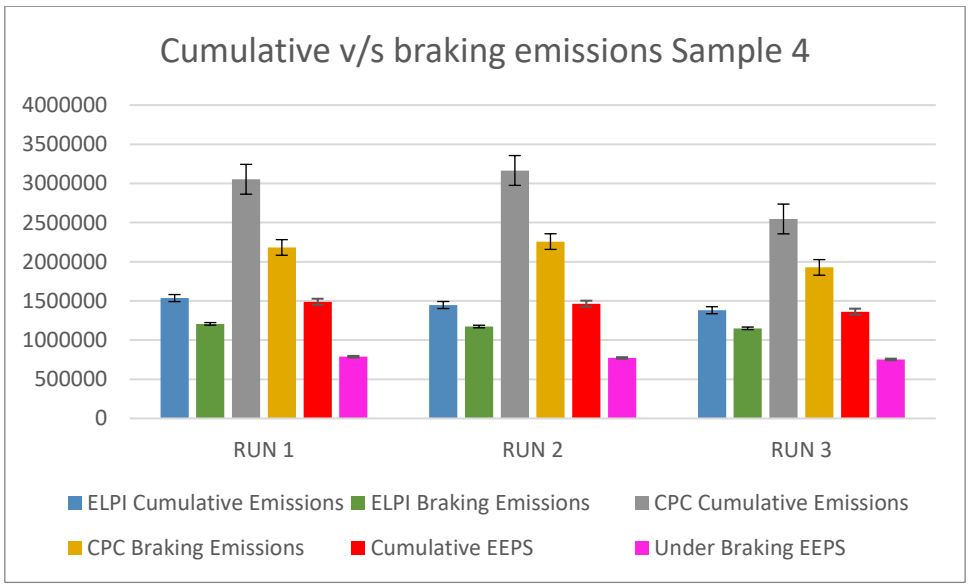

Figure 46. Cumulative concentrations over total runs compared with cumulative concentrations from braking events

The concentrations plotted in Figure 46 are tabulated in Tables 13-15, with the change between the complete run emission and that from braking events only being noted.

Table 13. Total Cumulative Concentrations measured by CPC for whole cycle and only under braking

CPC	Total Cumulative PN (#/cm^3)	Total Cumulative PN under braking (#/cm^3)	PN contribution of non-braking events (%)
RUN 1	3053095	2182679	28.5
RUN 2	3165457	2257772	28.6
RUN 3	2546460	1928092	24.2

Table 14. Total Cumulative Concentrations measured by ELPI for whole cycle and only under braking

ELPI	Total Cumulative PN (#/cm^3)	Total Cumulative PN under braking (#/cm^3)	PN contribution of non-braking events (%)
RUN 1	1536585	1207213	21.4
RUN 2	1447901	1173569	18.9
RUN 3	1381259	1150668	16.6

Table 15. Total Cumulative Concentrations measured by EEPS for whole cycle and only under braking

EEPS	Total Cumulative PN (#/cm^3)	Total Cumulative PN under braking (#/cm^3)	PN contribution of non-braking events (%)
RUN 1	1489443	788268.6	47.0
RUN 2	1464457	772069.5	47.2
RUN 3	1362652	753265.7	44.7

5.1.2 Repeatability of Particle Size Distribution

The size spectra of the particles emitted during the brake testing were estimated from the ELPI data. The repeatability here would be in the distribution of particles over different diameters emitted during the course of each run.

In Figure 47 below, we see the Particle Size Distribution (PSD) of Sample 1 over all the runs measured by EEPS. The A two-peak distribution is visible with all the runs showing a high degree of repeatability. Run 3 lags behind the other two runs as they approach the peak in the larger diameters range, and after this deviation, converges with the other curves.

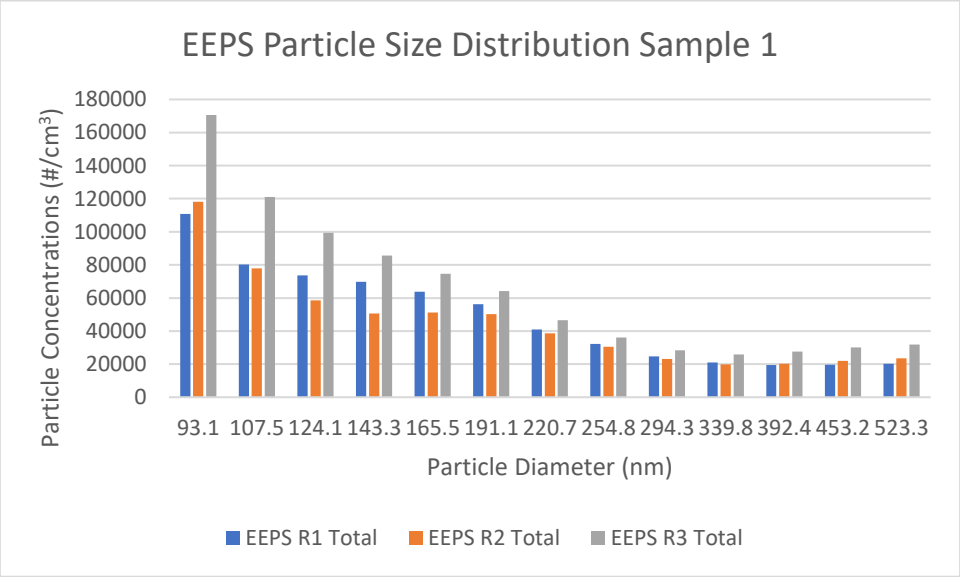

Figure 47. EEPS Size Distribution of Sample 1 over individual runs

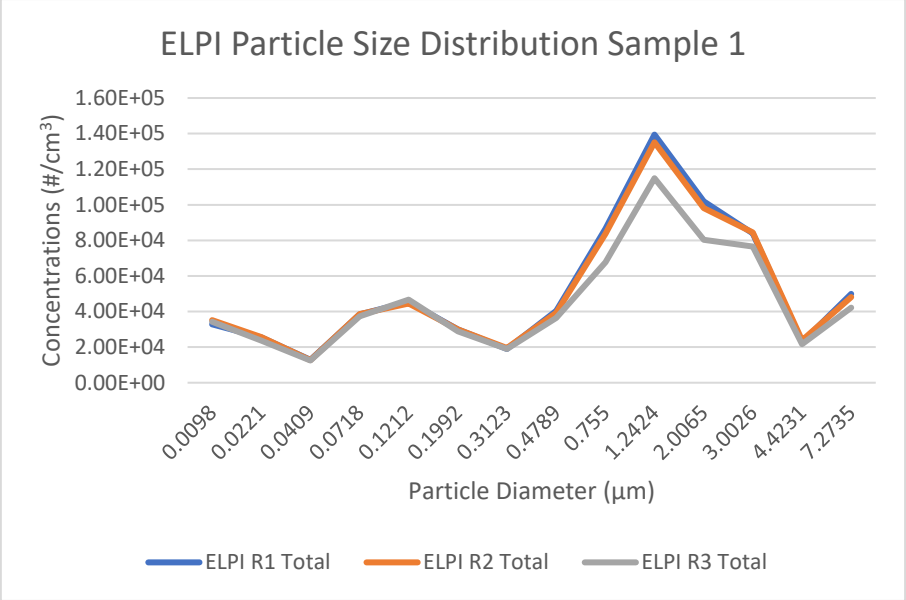

Figure 48. ELPI Size Distribution for Sample 1

Figure 48 shows the PSD for the same sample as measured by the ELPI. Here remarkable degree of repeatability is seen in the distribution in the smaller channels. The runs 1 and 2 show very similar concentrations in all the channels of the ELPI, with run 3 reporting a lower concentration at the channel of particle diameter 1.2424um.

In the Figures 49 and 50, we see the particle size distribution for sample 2 over the course of 3 runs of the WLTP brake cycle recorded by the EEPS and ELPI respectively.

To address the repeatability of the experiment for this sample, it is evident from the graph that the ELPI shows an almost uniform distribution of particles in diameters < 1µm between all the 3 runs. As the particle sizes increase, there is a marginal difference in the size distribution, with the first run reporting a relatively lower number of particles in the 1µm - 10µm range.

Figure 50 also shows a two-peak distribution in the range of particles with diameters <100 nm and >1 µm, which are consistent with experiments performed investigating particle size

distributions originating from brake wear [33][34][35], which is consistent across all the runs with good repeatability in the case of sample 2.

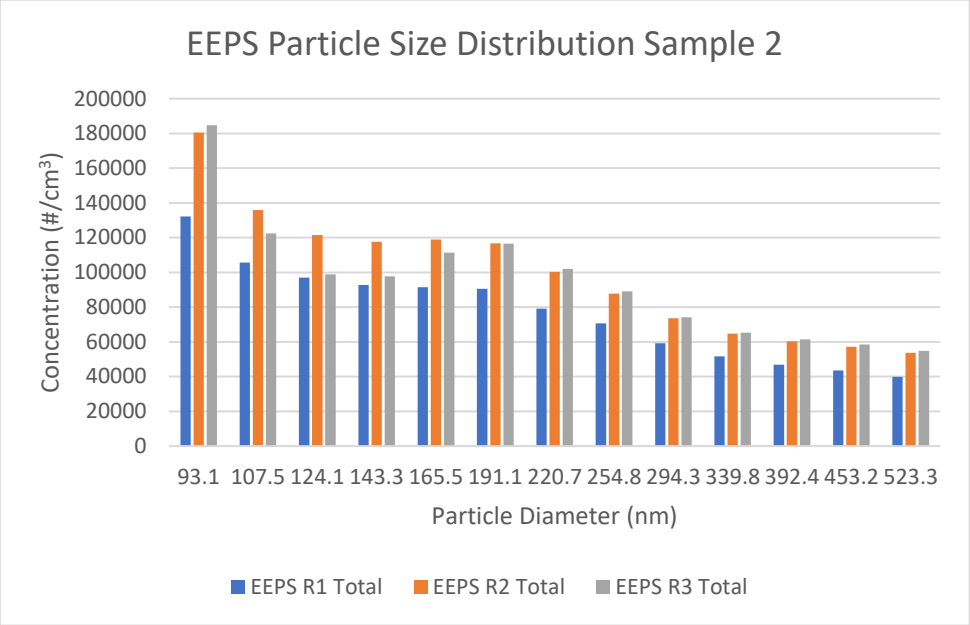

Figure 49. EEPS Size Distribution over each run for Sample 2

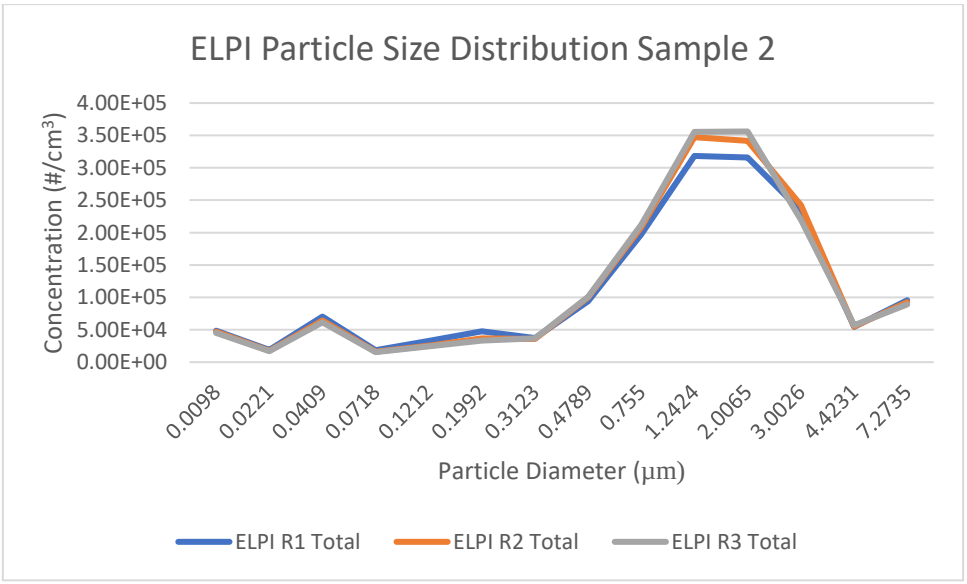

Figure 50. ELPI Particle Size Distribution for Sample 2

We see the size distribution over all the runs for the Sample 3 in Figure 51 as measured by the EEPS. As seen with the other samples, the EEPS records maximum PN concentrations in the smaller channels with the distribution reducing as the channel size increases. In Figure 52,

we have the particle size distribution measured by the ELPI. Unlike the other samples, the distribution curve for this sample does not show a clear peak in the region of particles with diameters < 0.1μm. Instead, the concentrations reduce in number as the particle size increases initially, before showing a maximum peak after 1 μm. The runs follow each other closely before deviating in concentrations as they approach the peak and then converge again.

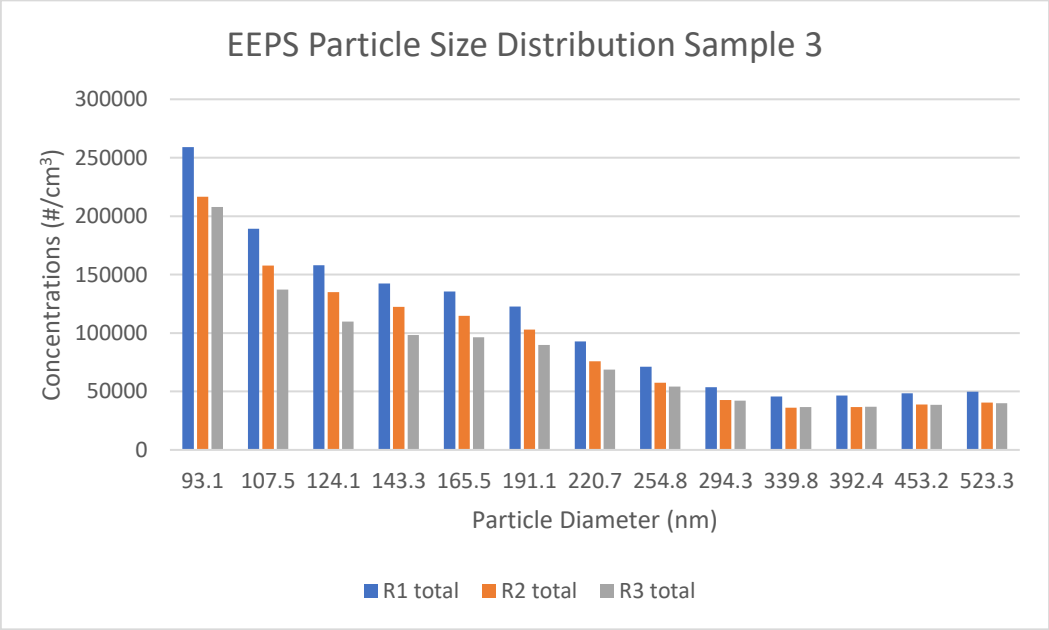

Figure 51. EEPS Particle Size Distribution of Sample 3 over all runs

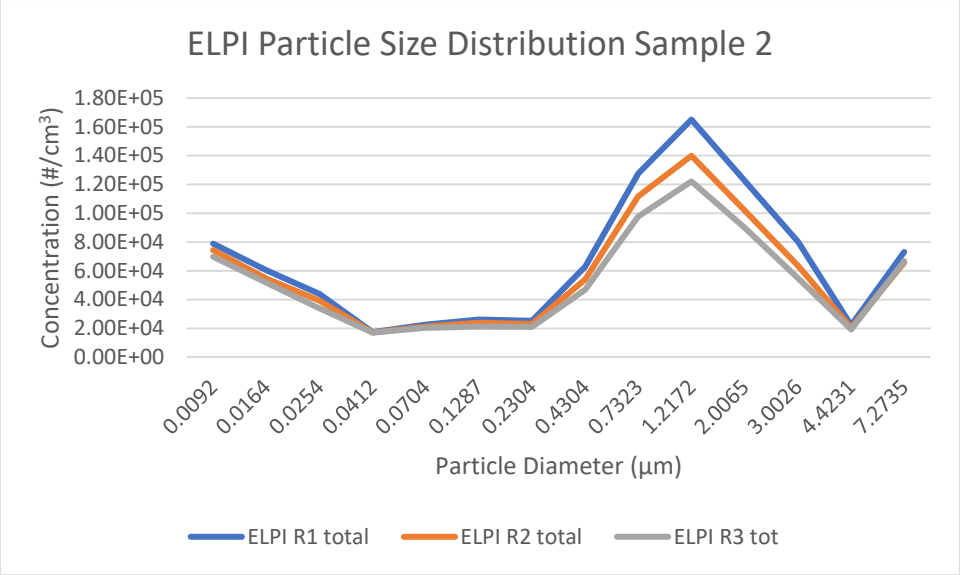

Figure 52. ELPI Particle Size Distribution for Sample 2 over all runs

Figures 53 and 54 show the size distribution curves for sample 4 compared over individual runs measured by the EEPS and ELPI respectively. Here, the repeatability is very good for measured particles over 1 µm in diameter for all the three runs seen in the measured data from ELPI. When the particles are smaller in size, the repeatability is disturbed slightly in the case of run 1.

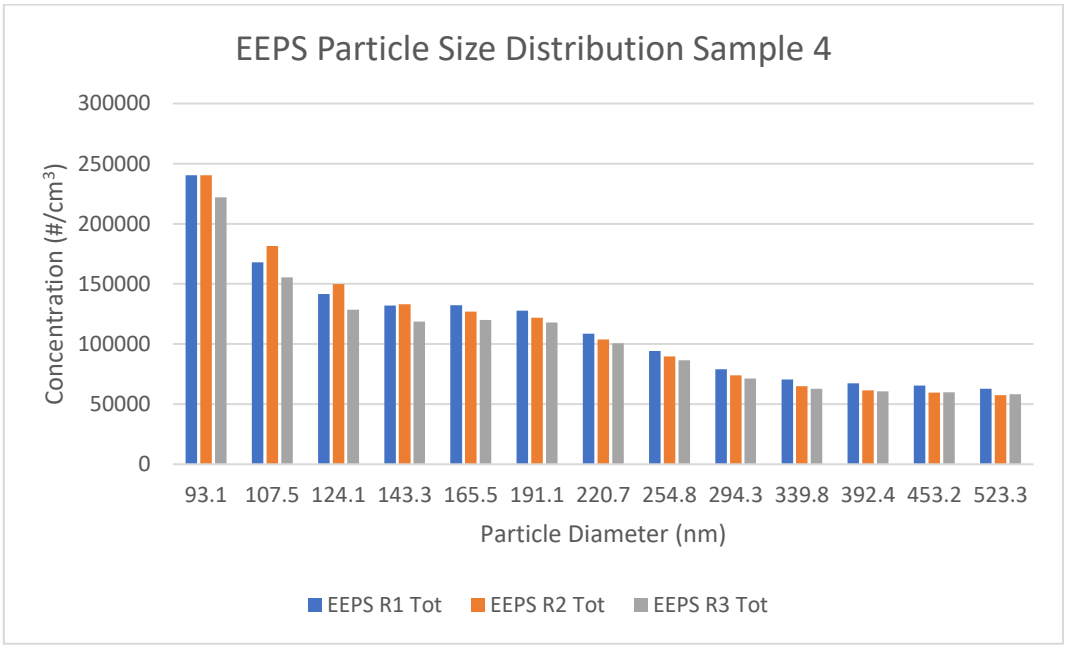

Figure 53. EEPS Particle Size Distribution over each run for Sample 4

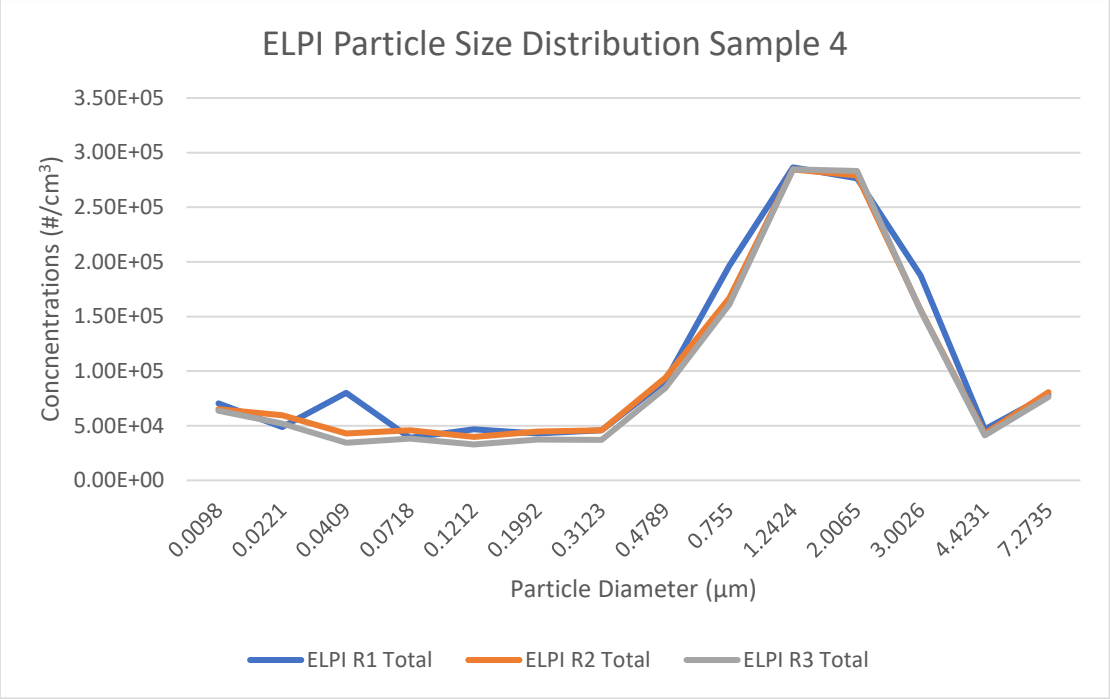

Figure 54. ELPI Particle Size Distribution over all runs for Sample 4

We also see that the two-peak distribution exhibited by Sample 2 has only been replicated with run 1. The other runs differ from run 1 in the <0.1 µm range but display consistent behaviour in the >1 µm range.

5.2 Effect of Brake Application on PN

Following the discussion in section 4.6, it was observed that the brake particles are generated even after the brakes have been fully released. This is the phenomenon of brake drag, wherein which the particles accumulated as secondary plateau shown in the Figure 9 as well as more particles generated from the gradual release of brake pressure continue to be detected by the instruments even with no brake pressure acting on the disc.

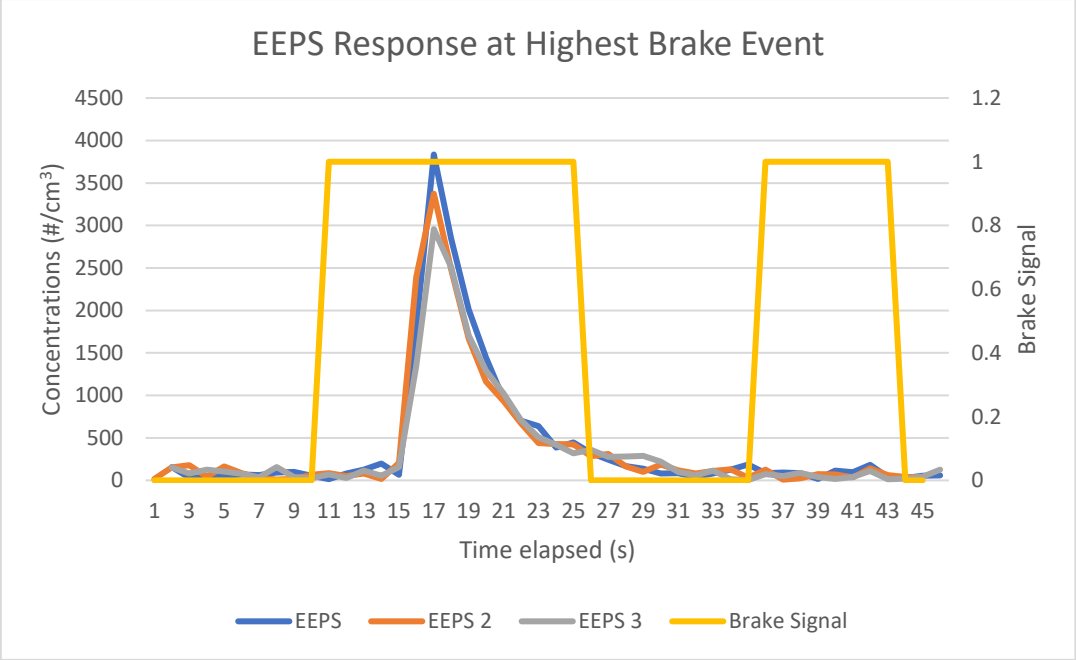

Figure 55. EEPS Signal at highest braking event

In the Figure 55, we see the response of the EEPS, measuring the concentrations in a short interval of 10 seconds before and 20 seconds after the braking event for the sample 3. Brake signal is taken from the voltage signal that is proportional to the braking pressure, shown here as a step response. From the figure, it is seen that there is still considerable particle generation (~10% of the maximum PN generated on brake application) even after the brake has been fully released and continues for a short duration, with the magnitude of particle generation reducing between successive runs.

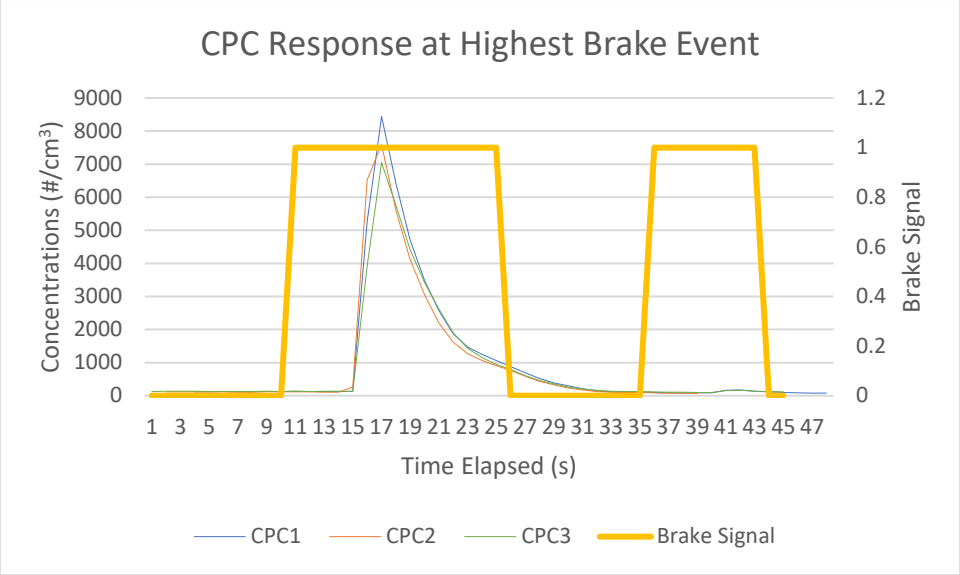

Figure 56. CPC Concentrations measured at highest braking event

Similar behaviour in terms of particle generation can be seen in the response of the CPC (Figure 56) as well, with particles appearing to be detected for a noticeable period after the brake is released.

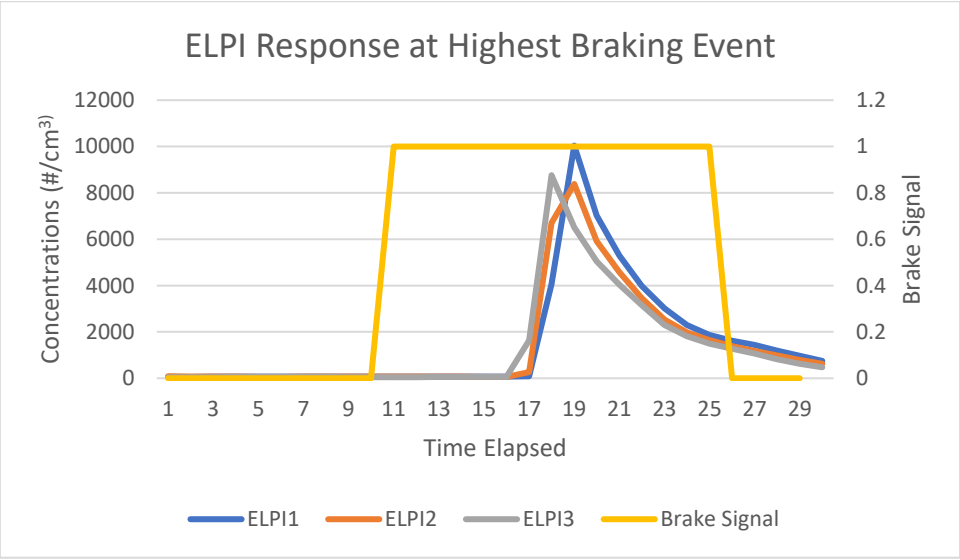

Figure 57. ELPI Concentrations at highest braking event

This phenomenon is again correlated by the ELPI in Figure 57 with ~10% of particles generated after the brakes are released.

The total cumulative PN emissions from the samples across all the cycles have been tabulated below. To quantify these emissions, the total emissions generated over the cycle for an individual brake must be calculated.

This is done by multiplying the flow rate in the chamber with the total cumulative PN concentration measured at the end of the run to obtain the total cumulative emissions per cycle. When this value is normalized with the driving distance of the cycle and the simulated vehicle mass on the brake, the total PN emitted per brake for each kilometre of driving is obtained. This can be seen in the equation below:

$$PN\left(\frac{\#}{\frac{km}{brake}}\right) = \frac{([\sum PN_{all\ channels}]\times Q)}{(S\times m_{simulated})}$$

Where, Q = flow rate through the tunnel = 2400 m^3/hr = 666666.7 cm^3/s

S = driving distance in the cycle = 192 km (WLTP Brake cycle)

$M_{simulated}$ = simulated mass on the tested brake, expressed as %/100 = 0.35 for this experiment

The results of the emissions of each sample recorded by the CPC and the ELPI is shown below.

Table 16. Estimated Total PN per brake measured by ELPI

ELPI	RUNS	Total Cumulative Concentrations (#/cm³)	Cumulative emissions per cycle (#/cycle)	Total cumulative emission per brake ((#/km)/brake)	Cumulative concentrations under Braking	Cumulative emissions per cycle under braking (#/cycle)	Total cumulative emission per brake ((#/km)/brake)
Sample 1	R1	728828	4.85E+11	7.22E+09	328568	2.19E+11	3.26E+09
	R2	718749	4.79E+11	7.13E+09	376863	2.51E+11	3.74E+09
	R3	641588	4.27E+11	6.35E+09	363860	2.43E+11	3.62E+09
Sample 2	R1	1583560	1.06E+12	1.58E+10	1301222	8.67E+11	1.29E+10
	R2	1629647	1.09E+12	1.62E+10	765718	5.10E+11	7.59E+09
	R3	1624365	1.08E+12	1.61E+10	714864	4.77E+11	7.10E+09
Sample 3	R1	927868	6.19E+11	9.21E+09	614434	4.09E+11	6.09E+09
	R2	810185	5.40E+11	8.04E+09	567052	3.78E+11	5.63E+09
	R3	731945	4.88E+11	7.26E+09	314245	2.09E+11	3.11E+09
Sample 4	R1	1536585	1.02E+12	1.52E+10	1207213	8.05E+11	1.20E+10
	R2	1447901	9.65E+11	1.44E+10	1173569	7.82E+11	1.16E+10
	R3	1381259	9.21E+11	1.37E+10	1150668	7.67E+11	1.14E+10

Table 17. Estimated Total PN per brake measured by CPC

CPC		Total Cumulative Concentrations (#/cm³)	Cumulative emissions per cycle (#/cycle)	Total cumulative emission per brake ((#/km)/brake)	Cumulative concentrations under Braking	Cumulative emissions per cycle under braking (#/cycle)	Total cumulative emission per brake ((#/km)/brake)
Sample 1	R1	904980	6.03E+11	8.97E+09	469445	3.12E+11	4.64E+09
	R2	791558	5.27E+11	7.84E+09	427215	2.84E+11	4.23E+09
	R3	788166	5.25E+11	7.81E+09	404190	2.69E+11	4.00E+09
Sample 2	R1	1674158	1.12E+12	1.67E+10	1120496	7.47E+11	1.11E+10
	R2	1719264	1.15E+12	1.71E+10	810504	5.40E+11	8.04E+09
	R3	1624501	1.08E+12	1.61E+10	752470	5.01E+11	7.46E+09
Sample 3	R1	1973642	1.32E+12	1.96E+10	914106	6.09E+11	9.06E+09
	R2	1729600	1.15E+12	1.71E+10	796809	5.31E+11	7.90E+09
	R3	1612229	1.07E+12	1.59E+10	733228	4.89E+11	7.28E+09
Sample 4	R1	3053095	2.04E+12	3.04E+10	2182679	1.46E+12	2.17E+10
	R2	3165457	2.11E+12	3.14E+10	2257772	1.51E+12	2.25E+10
	R3	2546460	1.70E+12	2.53E+10	1928092	1.29E+12	1.92E+10

5.3 Bedding In Process Runs

All the samples were subjected to an initial bedding-in process, consisting of 5 runs of the WLTP cycle, before the testing runs began. This is done to ensure optimal performance of the brakes and pads by depositing a layer of the pad material on the surface of the brake disc. Doing so increases the effective area of contact between the pads and the disc surface and consequently improves braking performance. The samples also resemble the real-world brake assembly conditions more closely after the bedding in process.

The data from the bedding in runs was not fully available owing to various circumstances, which gives limited useful signal, some of which is shown below.

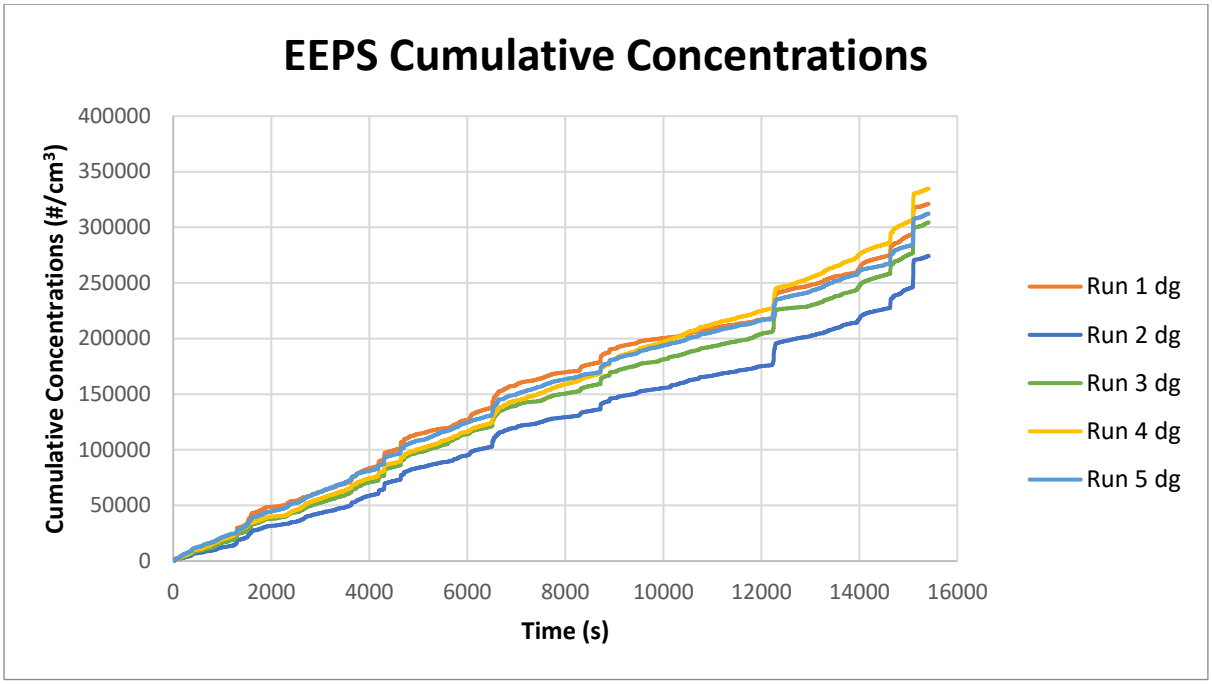

Figure 58. EEPS Cumulative Emissions during bedding-in runs of sample 2

Figure 58 shows the cumulative emissions measured over all 5 of the bedding-in runs for sample 2. All the runs show very good repeatability over the course of the run, with the curves for the runs being similar to each other and differing marginally in slope.

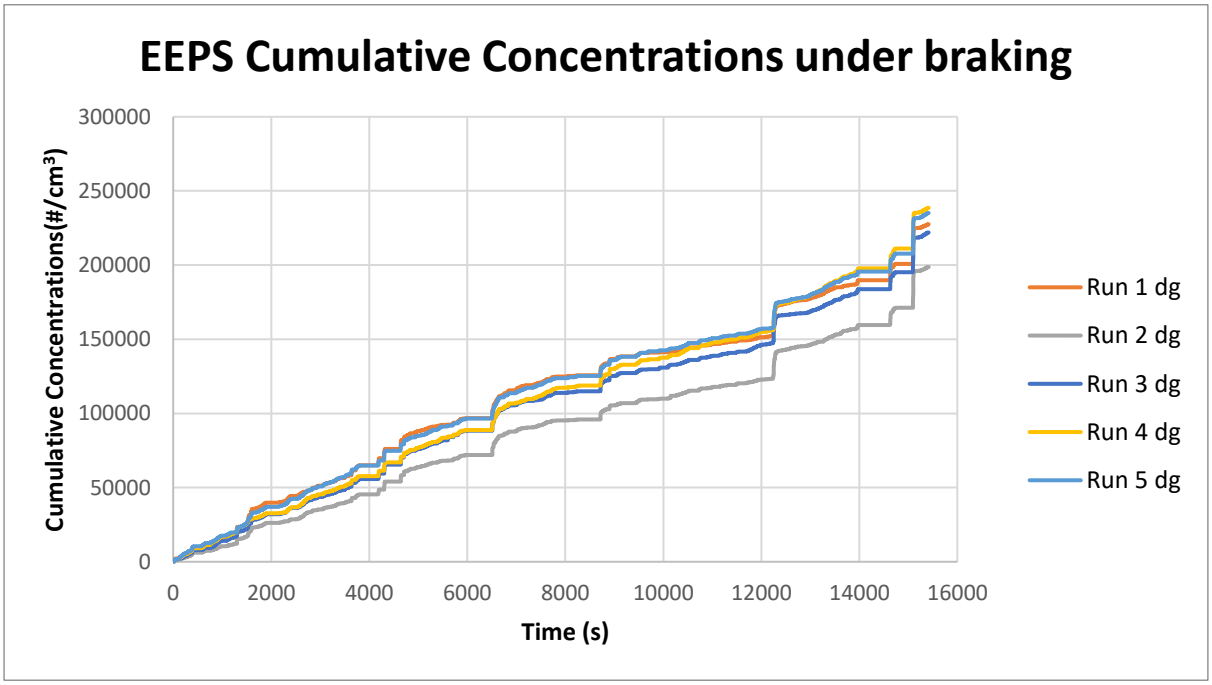

Figure 59. EEPS Cumulative Concentrations under braking for bedding in runs of sample 2

In Figure 59, we see that run 2 has a lower share of braking events contributing to the total cumulative PN. However, as seen for the total runs, the repeatability is good.

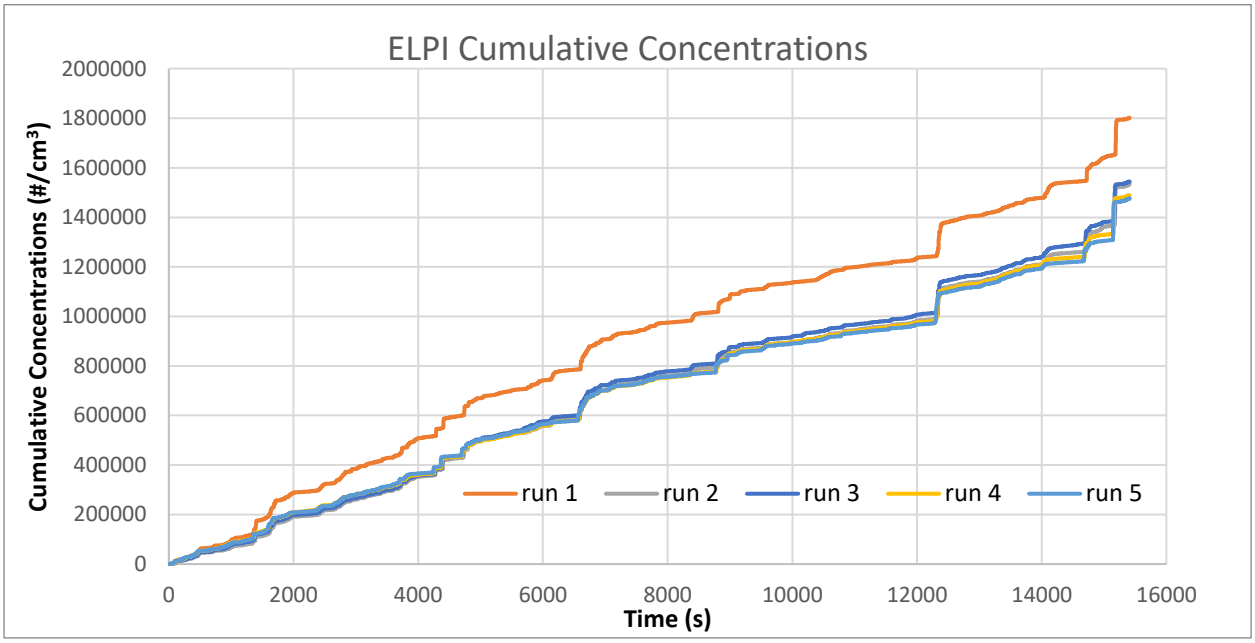

Figure 60. ELPI Cumulative Concentrations for bedding in runs

In Figure 60, cumulative concentrations measured by ELPI for bedding in runs of sample 2 are shown. Run 1 shows clear deviation in the slope, however, the other runs exhibit identical accumulation of particles.

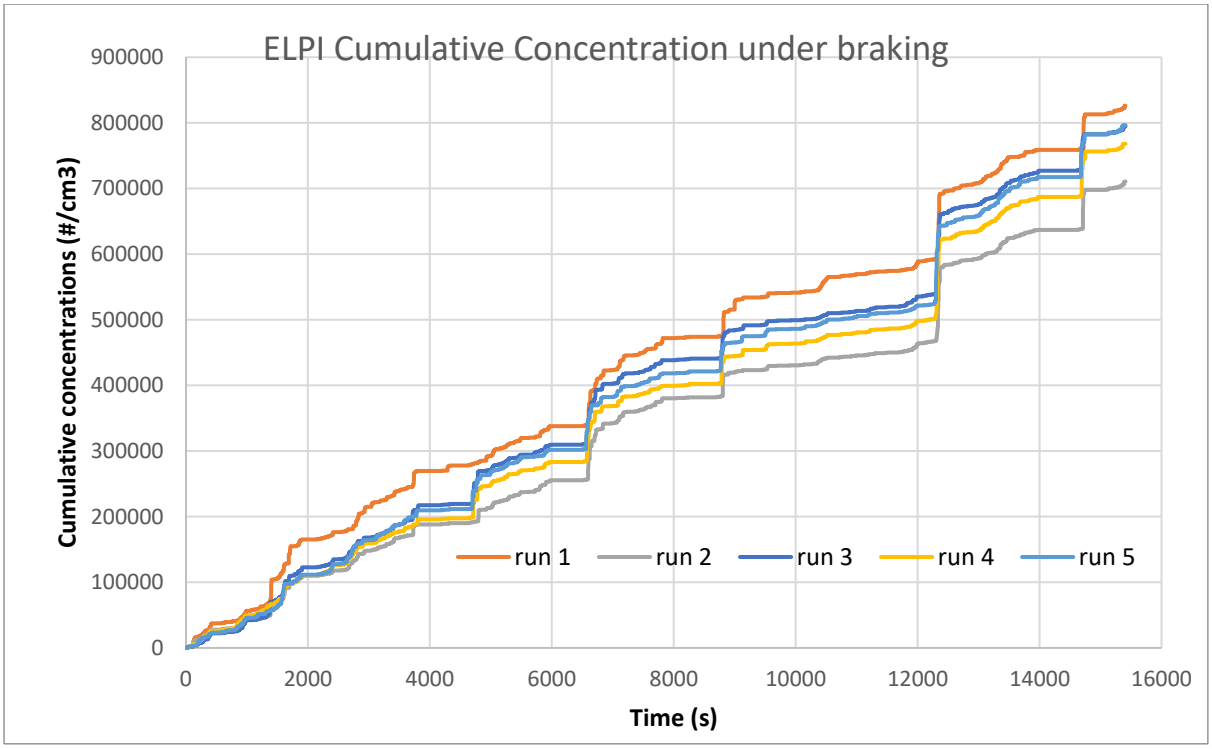

Figure 61. ELPI Cumulative Concentrations under braking for bedding in runs

Figure 61 shows the contribution of only braking events to the cumulative concentrations. From these figures, it is seen that sample 2 has displayed good repeatability as measured by both the EEPS and the ELPI in both braking and non-braking events contribution to total PN.

6. CONCLUSIONS

Non-exhaust emissions are gaining importance as the relative contribution of exhaust emissions to total Particulate matter emission is decreasing because of strict legislation on particles emitted from tail pipe which has limit of 6 x 10^{11} #/km on WLTC for light-duty vehicles. Brake wear particles produced during the newly developed brake cycle (WLTP Brake) were measured, with the four samples tested, consisting of combinations of two brake pads and two brake discs.

The data collected at the brake wear measurement campaign from ELPI, EEPS and a CPC were analysed after differentiating useful signal and unwanted noise by creating detection limit and eliminating background noise. Looking at the repeatability of experiment, we have observed that all the instruments have noted that the pattern of accumulation of particles over the course of the cycle is consistent between the different samples tested with some outliers.

Repeatable measurements (tabulated in Tables 4-15) were recorded in the experiment at the emission rates for each of the brakes, as calculated in Tables 16 and 17, which are relatively low. From the measured samples, the total PN that is emitted from an individual brake is in the range of magnitudes of 10^{9} and 10^{10} #/km. In comparison, the exhaust PN emissions limit is set at 6 x 10^{11} #/cm^{3}, an order of magnitude higher than the PN calculated during the runs.

It was also seen that there is a considerable amount (10% of the maximum particles generated when brake was applied) of particles generated by the effects of brake drag, and this effect was seen with reasonable consistency by the instruments. The cumulative concentrations generally followed the trend of showing reduced PN with successive runs.

The particle size distribution curves of all the samples have also shown very high degree of repeatability, with all samples exhibiting very similar distributions between runs. There are some variances between the curves of different samples, but the distributions have all a good repeatability.

There was a restriction with the EEPS as the lower channels could not be used to gather meaningful data and hence the reported concentrations by the EEPS are significantly lower in comparison with the ELPI and the CPC. The EEPS was able to identify particles with diameters over 90 nm. The ELPI and the CPC had no such issues and generally reported figures which are realistic to the drive cycle.

The bedding-in runs for the Sample 2 were also analysed and was seen that the experiment displays good repeatability of measurements even during the bedding-in process for the samples.

REFERENCES

1. World Health Organization – *Health topics – Air Pollution*

2. Thorpe, Alistair, and Roy M. Harrison. "Sources and properties of non-exhaust particulate matter from road traffic: a review." *Science of the total environment* 400.1-3 (2008): 270-282.

3. European Environmental Agency – *Air Quality in Europe 2022.* Available: https://www.eea.europa.eu/publications/air-quality-in-europe-2021/air-quality-status-briefing-2021

4. Amato, F. Dimiropoulos, A. and Farrow, K. – "Challenge, An Ignored Environmental Policy. "Non-exhaust Particulate Emissions from Road Transport." Available - https://www.actu-environnement.com/media/pdf/news-36643-rapport-ocde-emissions-hors-echappement.pdf

5. United States Environmental Protection Agency, "United States Environmental Protection Agency," [Online]. Available: https://cfpub.epa.gov/roe/indicator.cfm?i=9.

6. Mühlfeld. C, Rothen-Rutishauser. B, Blank. F, Vanhecke. D, Ochs. M and Gehr. P. (2008). Interactions of nanoparticles with pulmonary structures and cellular responses. American journal of physiology. Lung cellular and molecular physiology. 294. L817-29. 10.1152/ajplung.00442.2007.

7. Kelly, F. J. and Fussell, J. C. "Size, source and chemical composition as determinants of toxicity attributable," Atmospheric Environment, vol. 60, pp. 504-526, 2012.

8. Kefayati, S., Holdsworth, D.W. and Poepping, T.L., 2014. Turbulence intensity measurements using particle image velocimetry in diseased carotid artery models: Effect of stenosis severity, plaque eccentricity, and ulceration. *Journal of biomechanics*, *47*(1), pp.253-263.

9. B. D. Garg, S. H. Cadle and P. A. Mulawa, "Brake Wear Particulate Matter Emissions," Environmental Science & Technology, vol. 34, pp. 4463-4469, 2000.

10. Wahlström, J., Olander, L. and Olofsson, U., 2010. Size, shape, and elemental composition of airborne wear particles from disc brake materials. *Tribology Letters*, *38*(1), pp.15-24.

11. Singh, Vikas, et al. "High resolution vehicular PM10 emissions over megacity Delhi: Relative contributions of exhaust and non-exhaust sources." *Science of the Total Environment* 699 (2020): 134273.

12. Kreider, Marisa L., et al. "Physical and chemical characterization of tire-related particles: Comparison of particles generated using different methodologies." *Science of the Total Environment* 408.3 (2010): 652-659.

13. Boulter, P. G., et al. "Road vehicle non-exhaust particulate matter: Final report on emission modelling." *Published project report PPR110* (2006).

14. Continental Reifen Deutschland GmbH . Tyre Basics - Passenger Car Tyres. TDC 11/2011 0130 1607, (2012) [Accessed: 12 June 2022]

15. Amato, Fulvio, ed. *Non-exhaust emissions: an urban air quality problem for public health; impact and mitigation measures*. Academic Press, 2018.

16. Gasser M, Riediker M, Mueller L, Perrenoud A, Blank F, Gehr P, Rothen-Rutishauser B (2009) Toxic effects of brake wear particles on epithelial lung cells in vitro. Part Fibre Toxicol 6(30)

17. Sanders PG, Xu N, Dalka TM, Maricq MM. Airborne brake wear debris: size distributions, composition, and a comparison of dynamometer and vehicle tests. *Environ Sci Technol.* 2003;37:4060–4069. doi: 10.1021/es034145s. [Accessed: 10 June 2022]

18. Grigoratos, T, and Giorgio M. "Brake wear particle emissions: a review." *Environmental Science and Pollution Research* 22.4 (2015): 2491-2504. [Accessed: 27 June 2022]

19. Palla, S. *Drum Brakes vs Disc Brakes* – Available: www.spinny.com/blog/index.php/drum-brakes-vs-disc-brakes [Accessed: 19 July 2022]

20. Thorpe, A. and Harrison, R. M. "Sources and properties of non-exhaust particulate matter from road traffic: a review," SCIENCE OF THE TOTAL ENVIRONMENT, vol. 400, pp. 270-282, 2008.

21. Bukowiecki, N. and Gehrig, R. "PM10 emission factors of abrasion particles from road traffic (APART)," in Swiss Association of Road and Transportation Experts (VSS), 2009.

22. Eriksson M, Bergman F, Jacobson S. 2002. On the nature of tribological contact in automotive brakes. Wear, 252(1-2), 26-36.

23. Zum Hagen, Ferdinand H. Farwick, et al. "Study of brake wear particle emissions: impact of braking and cruising conditions." *Environmental science & technology* 53.9 (2019): 5143-5150.

24. Andrew, M. *Brake Dynamometer Testing* – Available: https://www.brakeandfrontend.com/brake-dynamometer-testing-one-test-is-worth-a-thousand-expert-opinions/ [Accessed: 20 July 2022]

25. TSI, "EEPS," [Online]. Available: https://tsi.com/getmedia/a01ec52e-f39f-4312-8f9a-fded71631a69/3090_Engine_Exhaust_Particle_Sizer_A4_2980351_WEB?ext=.pdf [Accessed: 29 July 2022]

26. Centre for Atmospheric Science – *Condensation Particle Counters (CPC)* – Available: http://www.cas.manchester.ac.uk/restools/instruments/aerosol/cpc/ [Accessed: 29 July 2022]

27. Dekati, "ELPI," [Online]. Available: https://www.dekati.com/products/elpi/ [Accessed: 29 July 2022]

28. Woo, Sang-Hee, et al. "Characterization of brake particles emitted from non-asbestos organic and low-metallic brake pads under normal and harsh braking conditions." *Atmospheric Environment* 278 (2022): 119089.

29. Mathissen, M. and Grochowicz, J. "A novel real-world braking cycle for studying brake wear particle emissions," Wear, Vols. 414-415, pp. 219-226, 2018.

30. Black hills state university, [Online]. Available: https://www.bhsu.edu/Portals/91/InstrumentalAnalysis/StudyHelp/LectureNotes/Chapter5.pdf [Accessed: 6 August 2022]

31. Theodorsson, E., 2008. Limit of detection, limit of quantification and limit of blank. *Clinical biochemist review*, *29*, pp.1-39. [Accessed: 6 August 2022]

32. López, P., Szilágyi, S., Lerda, D. and Wenzl, T., 2009. Current approaches to determine limit of detection and limit of quantification. *Institute for reference meterials and measurements, JRC European commission*.

33. Hinds, W.C. and Zhu, Y., 2022. *Aerosol technology: properties, behavior, and measurement of airborne particles*. John Wiley & Sons.

34. Iijima, Akihiro, et al. "Particle size and composition distribution analysis of automotive brake abrasion dusts for the evaluation of antimony sources of airborne particulate matter." *Atmospheric Environment* 41.23 (2007): 4908-4919.

35. Hagino, Hiroyuki, Motoaki Oyama, and Sousuke Sasaki. "Airborne brake wear particle emission due to braking and accelerating." *Wear* 334 (2015): 44-48.

36. Hagino, Hiroyuki, Motoaki Oyama, and Sousuke Sasaki. "Laboratory testing of airborne brake wear particle emissions using a dynamometer system under urban city driving cycles." *Atmospheric Environment* 131 (2016): 269-278.

LIST OF FIGURES

LIST OF TABLES

APPENDIX

EEPS Bin Designations				
Bin number	Bin Min Dp (nm)	Bin Midpoint Dp(nm)	Bin Max Dp (nm)	dlogDp
B1	5.61	6.04	6.48	0.06
B2	6.48	6.98	7.48	0.06
B3	7.48	8.06	8.64	0.06
B4	8.64	8.06	9.98	0.06
B5	9.98	9.31	11.52	0.06
B6	11.52	10.75	13.3	0.06
B7	13.3	12.41	15.36	0.06
B8	15.36	14.33	17.74	0.06
B9	17.74	16.55	20.48	0.06
B10	20.48	19.11	23.65	0.06
B11	23.65	22.065	27.31	0.06
B12	27.31	25.48	31.54	0.06
B13	31.54	29.42	36.42	0.06
B14	36.42	33.98	42.06	0.06
B15	42.06	39.24	48.57	0.06
B16	48.57	45.31	56.09	0.06
B17	56.09	52.33	64.77	0.06
B18	64.77	60.43	74.79	0.06
B19	74.79	69.78	86.37	0.06
B20	86.37	80.58	99.74	0.06
B21	99.74	93.05	115.18	0.06
B22	115.18	107.46	133	0.06
B23	133	124.09	153.59	0.06
B24	153.59	143.29	177.37	0.06
B25	177.37	165.48	204.82	0.06
B26	204.82	191.09	236.52	0.06
B27	236.52	220.67	273.13	0.06
B28	273.13	254.82	315.41	0.06
B29	315.41	294.27	364.23	0.06
B30	364.23	339.82	420.61	0.06
B31	420.61	453.16	485.71	0.06
B32	485.71	523.23	560.89	0.06

ELPI Bin Designations			
Bin Number	D50% Lower cutoff (µm)	D50% upper cutoff (µm)	dlogDp
B14	5.3	10	0.28
B13	3.6	5.3	0.17
B12	2.5	3.6	0.16
B11	1.6	2.5	0.19
B10	0.94	1.6	0.23
B9	0.6	0.94	0.19
B8	0.38	0.6	0.2
B7	0.25	0.38	0.18
B6	0.15	0.25	0.22
B5	0.094	0.15	0.2
B4	0.054	0.094	0.24
B3	0.03	0.054	0.26
B2	0.016	0.03	0.27
B1	0.006	0.016	0.43

EEPS Instrument Specifications

Particle Size Range	5.6 to 560 nm
Particle Size Resolution	16 channels per decade (32 total)
Electrometer Channels	22
Charger Mode of Operation	Unipolar diffusion charger
Inlet Cyclone 50% Cut point	1 µm
Time Resolution	10 size distributions/sec
Sample Flow	10 L/min
Sheath Air	40 L/min
Inlet Sample Temperature	10 to 52°C
Operating Temperature	0 to 40°C
Storage Temperature	-20 to 50°C
Atmospheric Pressure Correction Range	70 to 103 kPa (700 to 1034 mbar)
Humidity	0 to 90% RH (noncondensing)
Computer Requirements	Pentium 4 processor, 2 GHz speed or better, at least 512 MB RAM
Power Requirements	100 to 240 VAC, 50/60 Hz, 250W

ELPI Instrument Specifications

Particle size range	0.006 - 10 µm
Number of channels	14 electrically detected + preseparator stage
Sampling rate	10 Hz
Nominal air flow	10 l/min
Ambient temperature	10-35 ° C
Sample conditions gas temperature	< 60 ° C
Electric power	100-250 V, 50-60 Hz, 200 W
Charger voltage	3.5 kV +/- 0.5 kV
Charger current	1 µA
Pump requirements	Minimum 16 m3/h @ 40 mbar
Computer requirements	MS-Windows 7, MS-Windows 8, MS-Windows 10
Connection to PC	RS-232 or Ethernet
3 analogue inputs	0-10 V
6 analogue outputs	0-10 V